

Structure-Based Design, Synthesis, and in vitro Evaluation of Bisubstrate Inhibitors for Catechol *O*-Methyltransferase (COMT)

Birgit Masjost,^[a] Patrick Ballmer,^[a] Edilio Borroni,^[b] Gerhard Zürcher,^[b] Fritz K. Winkler,^[b] Roland Jakob-Roetne,^[b] and François Diederich*^[a]

Abstract: The enzyme catechol *O*-methyltransferase (COMT) catalyzes the Me group transfer from the cofactor *S*-adenosylmethionine (SAM) to the hydroxy group of catechol substrates. Potential bisubstrate inhibitors of COMT were developed by structure-based design and synthesized. The compounds were tested for in vitro inhibitory activity against COMT obtained

from rat liver, and the inhibition kinetics were examined with regard to the binding sites of cofactor and substrate. One of the designed molecules was found to

be a bisubstrate inhibitor of COMT with an $IC_{50} = 2 \mu\text{M}$. It exhibits competitive kinetics for the SAM and noncompetitive kinetics for the catechol binding site. Useful structure–activity relationships were established which provide important guidelines for the design of future generations of bisubstrate inhibitors of COMT.

Keywords: catechol *O*-methyltransferase • chemical biology • drug research • enzyme inhibitors • structure-based design

Introduction

Inhibition of catechol *O*-methyltransferase (COMT) is an important approach for developing new therapeutic treatments in Parkinson's disease. COMT catalyzes a major deactivation pathway for catechol-based neurotransmitters such as dopamine. It is part of the metabolism of neurotransmitters known as "uptake 2" following the signal transfer by the neurotransmitter between the synaptic clefts of nerve cells.^[1, 2]

The symptoms of Parkinson's disease are a consequence of reduced levels of dopamine in the brain due to degeneration of the dopaminergic neurons. The current therapy consists of an artificial increase of the dopamine concentration by oral administration of a preparation of the amino acid L-DOPA and inhibitors of the enzyme aromatic amino acid decarboxylase (AAD) which avoid the degradation of L-DOPA in the periphery. Although L-DOPA can cross the blood brain barrier, dopamine and AAD inhibitors can not. In the brain, L-DOPA is decarboxylated by AAD to give dopamine. When

AAD is inhibited, deactivation by COMT becomes the major metabolic pathway for L-DOPA in the periphery. Inhibition of COMT reduces the peripheral degradation of L-DOPA and increases its supply into the brain.^[1]

COMT catalyzes the transfer of a Me group from its cofactor *S*-adenosylmethionine (SAM) to one HO group of catechols such as dopamine in an S_N2 -type reaction. The reaction is dependent on Mg^{2+} ions and involves binding of the catechol substrate to this ion at the active site of COMT. In mechanistic studies, it was found that binding of the cofactor SAM to the Mg^{2+} -enzyme complex occurs prior to binding of the catechol substrate.^[2, 3]

For decades, medicinal chemists in both industry and academia have searched for inhibitors of the catechol binding site of COMT.^[4–7] Two inhibitors, which both contain a 3-nitrocatechol group as the central structural unit, tolcapone (Tasmar[®])^[6] and entacapone (Comtan[®])^[8] have been developed into pharmaceuticals and introduced to the market recently. The fact that both compounds, which show inhibitory activity in the submicromolar concentration range, contain a catechol group reinforces the proposition that the catechol motif is crucial for the recognition between the enzyme and natural substrates such as dopamine.

Analogues of SAM have also been synthesized and their inhibitory activity on COMT studied, although to date no inhibitors with a $K_i < 10 \mu\text{M}$ have been reported.^[9–12] Of course, in this approach enzyme selectivity would be a major issue since the cofactor SAM exhibits a multitude of roles in the body.

[a] Prof. F. Diederich, B. Masjost, P. Ballmer
Laboratorium für Organische Chemie, ETH-Zentrum
Universitätstrasse 16, 8092 Zürich (Switzerland)
Fax: (+41) 1-632-1109

[b] Dr. E. Borroni, Dr. G. Zürcher, Dr. F. K. Winkler, Dr. R. Jakob-Roetne
Pharma Division, Präklinische Forschung
F. Hoffmann-La Roche AG
4002 Basel (Switzerland)

COMT has also been studied as a potential target for bisubstrate inhibitors replacing both the cofactor SAM and the catechol substrate.^[13–15] Bisubstrate inhibitors of enzymes such as spermidine synthase,^[16] farnesyl transferase,^[17] vaccinia RNA guanine 7-methyltransferase,^[18] and indole *N*-methyltransferase^[19] have been shown to display, in many cases, higher affinities than inhibitors mimicking only one substrate. However, no lead structure for a bisubstrate inhibitor of COMT has been reported.

The determination of the crystal structure of COMT^[20, 21] as a complex with SAM, 3,5-dinitrocatechol, and a Mg²⁺ ion opened the possibility for the rational design of bisubstrate inhibitors. The success of computer-assisted, structure-based design of enzyme inhibitors^[22, 23] depends on many parameters such as the quality of the X-ray crystal structure analysis, the conformational homogeneity of the enzyme active site, and a detailed knowledge of the catalytic mechanism.^[24] Here we describe the rational design, synthesis, and *in vitro* inhibitory activity of a bisubstrate inhibitor of COMT.

Results

Design of potential bisubstrate inhibitors: The crystal structure of COMT complexed with Mg²⁺, 3,5-dinitrocatechol, and SAM^[20] (Figure 1a) was analyzed for intermolecular bonding contacts between the amino acid residues of the enzyme and the three bound components. Figure 1b shows a schematic representation of the hydrogen bonding and Coulombic interactions in the quaternary complex. Three binding pockets were defined: one, which binds the catechol, is situated on the surface of the enzyme; it will be referred to as the catechol pocket. It contains the Mg²⁺ ion octahedrally coordinated to Asp141, Asp169, Asn170, one localized H₂O molecule, and the two HO groups of the catechol, one of which is deprotonated under

physiological conditions (pH 7). The second binding pocket contains the ribose moiety and a third the adenine base of the SAM cofactor; they will be referred to as ribose and base pockets, respectively, and are more embedded in the enzyme. In particular, Trp143 shields the bound nucleoside portion of SAM from the enzyme surface. The two ribose HO groups interact with the COO⁻ residue of Glu90, and the adenine moiety is bound via a characteristic hydrogen bonding array

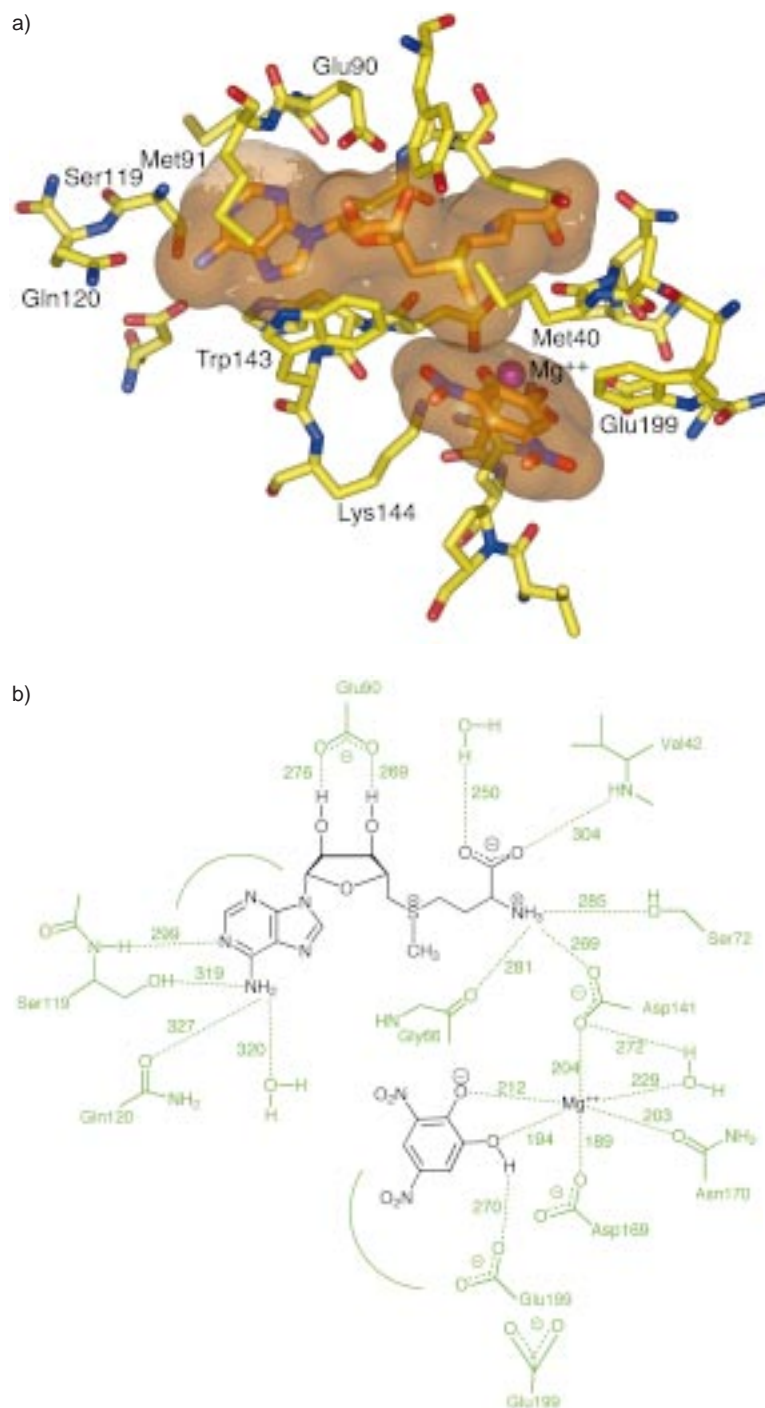


Figure 1. a) Cofactor SAM, 3,5-dinitrocatechol, and Mg²⁺ ion situated in the active site of COMT as found in the X-ray crystal structure of recombinant rat COMT, see [20]. The Connolly surfaces of SAM and 3,5-dinitrocatechol are shown. b) Schematic drawing of the active site of COMT and its hydrogen bonding and Coulombic interactions with the two substrates and the Mg²⁺ ion. Distances in pm.

to the protein. Its NH₂ group forms hydrogen bonds to Gln120 and a fixed H₂O molecule while it accepts a hydrogen bond from the HO group of Ser119. The latter amino acid also forms an essential hydrogen bond with its backbone N-H group to N(1) of the nucleobase. The methionine part of SAM binds to a channel-like opening in the enzyme made from polar amino acid residues.

The design of the bisubstrate inhibitors was performed by computational methods, using the programs MOLOC,^[25] Insight II,^[26] and MacroModel.^[27] The hypothesis was made that the highly polar methionine channel would be favorably filled with water in the presence of an inhibitor which would only occupy the remaining three binding pockets. Therefore, in the design of a bisubstrate inhibitor, a potential occupation of the methionine channel was neglected, which turned out to be a remarkably successful structural simplification. We subsequently chose to construct the potential inhibitor by connecting the C(5′)-OH group of adenosine (as in SAM) or adenosine substitutes via an appropriate spacer to a suitable catechol moiety, thereby filling the adenine, ribose, and catechol binding pockets. We hoped to preserve in the complex formed by the bisubstrate inhibitor in the presence of Mg²⁺ all the directional hydrogen bonding and Coulombic interactions schematically shown in Figure 1b.

Potent enzyme inhibition by catechols is known to require that the p*K*_A of one of the two HO groups is sufficiently lowered to ensure deprotonation at physiological pH.^[4] Therefore, we chose a catechol derivative in which one HO group is acidified by a *p*-NO₂ group and an *o*-carboxamide group which, at the same time, acts as the anchor for the connection to the nucleoside moiety.

To ensure that the catechol and nucleoside moieties of the bound bisubstrate inhibitor would benefit of all the directional interactions seen in the X-ray crystal structure of the quaternary complex (COMT, SAM, 3,5-dinitrocatechol, Mg²⁺), the nature of the connecting bridge between these moieties needed to be optimized. Extensive modeling showed the ribose-C(5′)-O-CH₂-CH₂-NH-CO-catechol linker in **1**, with a planar *trans* amide group, to meet best the

sensitive length and shape requirements for this bridge. Figure 2a displays the most favorable conformation of **1** docked into the X-ray crystal structure of COMT. This structure was obtained by energy minimization of the inhibitor inside the enzyme whose coordinates (including the Mg²⁺ ion) were fixed. Figure 2b provides a schematic view of the bonding interactions in the modeled ternary complex between COMT, Mg²⁺ ion, and **1**. As is readily apparent from a comparison between Figures 1 and 2, all directional hydrogen bonding and Coulombic interactions seen in the X-ray crystal structure of the quaternary complex with SAM and 3,5-dinitrocatechol are maintained in the modeled structure with the bound potential bisubstrate inhibitor. The bridge N-CH₂-CH₂-O-CH₂ between catechol and ribose features a sequence of favorable *ap* (*antiperiplanar*)-*ap-sc* (*synclinal*)-*sc* (*synclinal*) torsional angles. The computational analysis revealed 25 short contacts (<3.7 Å) and no repulsive interactions between enzyme and inhibitor.

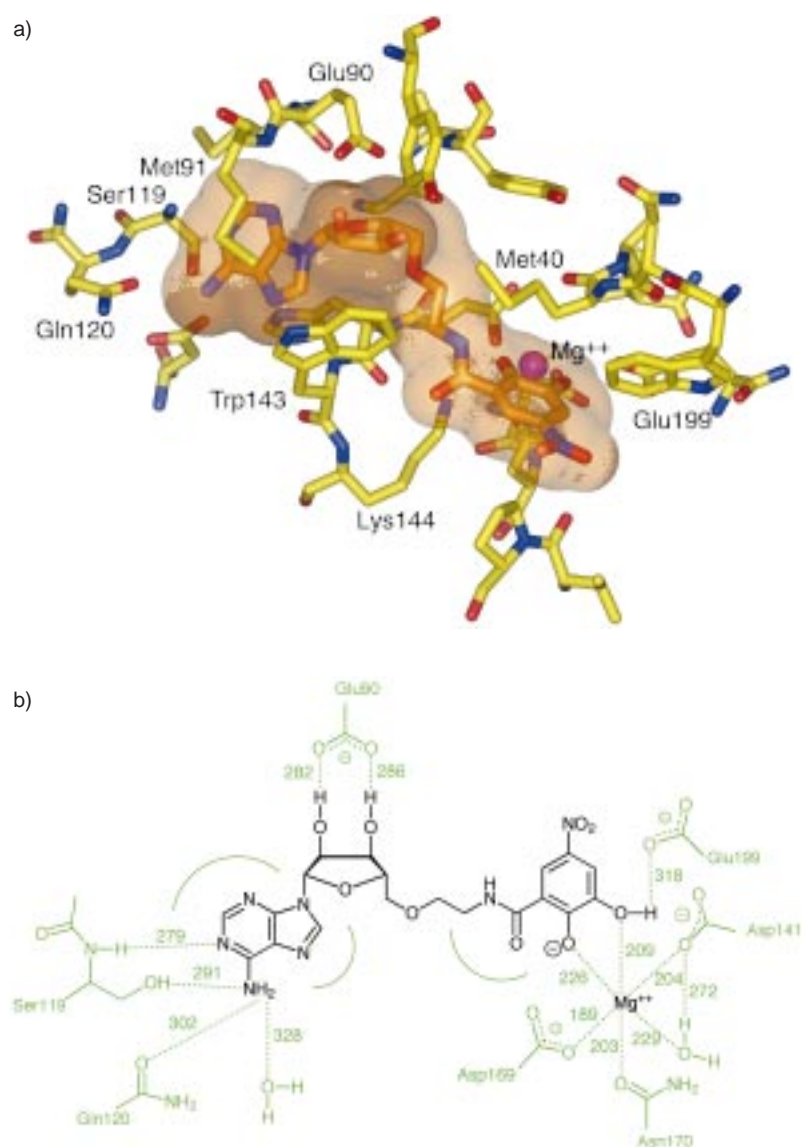
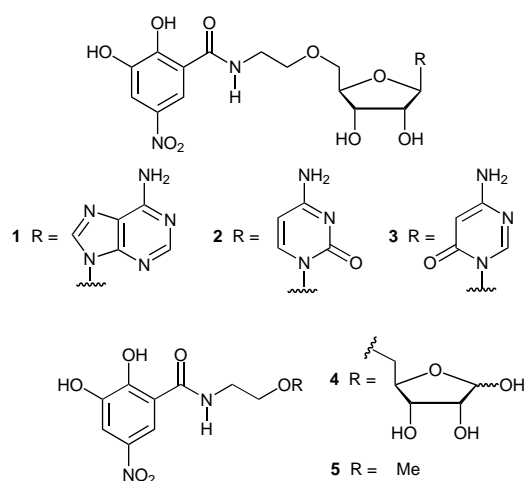


Figure 2. a) Computer-modeled ternary complex between COMT, Mg²⁺ and bisubstrate inhibitor **1**. The Connolly surface of the inhibitor is shown. b) Schematic drawing of the directional interactions in the modeled ternary complex. Distances in pm.



We also considered **2** and **3** containing cytosine and 6-amino-3,4-dihydropyrimidin-4-one as adenine substitutes, respectively, as potential bisubstrate inhibitors. Figure 3 provides a schematic drawing of the hydrogen bonding

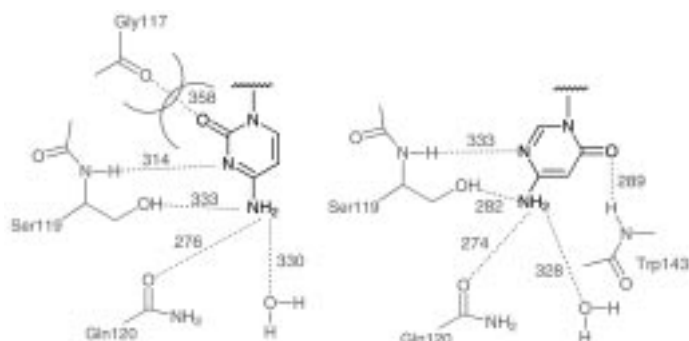
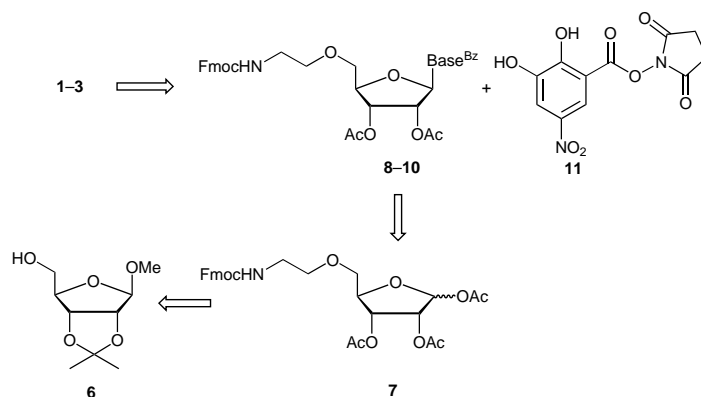


Figure 3. Left: Schematic drawing of the interactions of the cytosine base of **2** in the modeled complex with COMT. Right: Schematic drawing of the interactions of the 6-amino-3,4-dihydropyrimidin-4-one moiety of **3** in the modeled complex with COMT. Distances in pm.

interactions of the bases in the two compounds docked into COMT. While the hydrogen bonding arrays resemble those seen in the modeled complex of **1** (Figure 2b), an unfavorable contact between the carbonyl O-atoms of Gly117 and cytosine was observed in the modeled complex of **2**. In the complex of **3**, an additional hydrogen bond was found between the pyrimidinone C=O group and the backbone N-H of Trp143. The intermolecular interactions involving the ribose and catechol moieties are similar in the predicted complexes of all three potential bisubstrate inhibitors **1–3**. Compounds **4** and **5** lacking the nucleobase and the entire nucleoside portion, respectively, were also included for comparison in this study.

Synthesis: For the synthesis of **1–3**, a general approach was chosen that allows the introduc-

tion of different natural and modified bases^[28–32] into the ribose moiety in a regio- and stereoselective fashion (Scheme 1). The sequence starts from commercially available 2,3-*O*-isopropylidene- β -D-ribose (**6**) which is transformed into the Fmoc protected [Fmoc = (9*H*-fluoren-9-ylmethoxy)carbonyl], acetylated ribose derivative **7** and, by nucleosidation

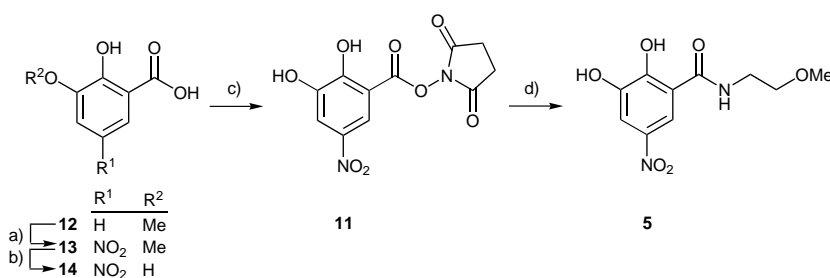


Scheme 1. General synthetic route to the potential bisubstrate inhibitors of COMT. Fmoc = (9*H*-fluoren-9-ylmethoxy)carbonyl. Base^{Bz} = *N*-benzoyl protected nucleobase.

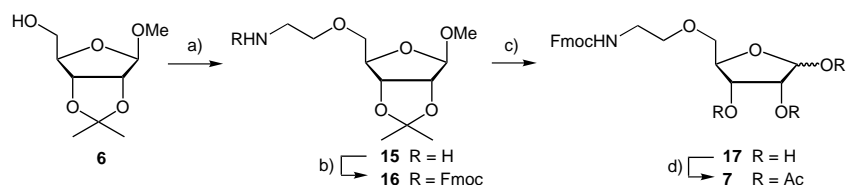
with *N*-benzoyl protected bases, into nucleosides **8–10**. Coupling of Fmoc deprotected **8–10** with the activated catechol derivative **11** to the target compounds **1–3** was performed at the end of the synthesis, because nucleosidation of ribose derivatives already containing the catechol moiety was not successful.

For the preparation of the activated catechol derivative **11**, commercially available 2-hydroxy-3-methoxybenzoic acid (**12**) was nitrated under standard conditions to give regioselectively **13** (94% yield) (Scheme 2). Demethylation with 40% aqueous HBr afforded nitrocatechol **14**^[33] (79%) which was purified by sublimation. Reaction of **14** with *N*-hydroxysuccinimide (HOSu) in the presence of DCC (*N,N'*-dicyclohexylcarbodiimide) afforded the activated ester **11** (53%). Coupling of **11** with 2-methoxyethylamine provided compound **5** in 75% yield.

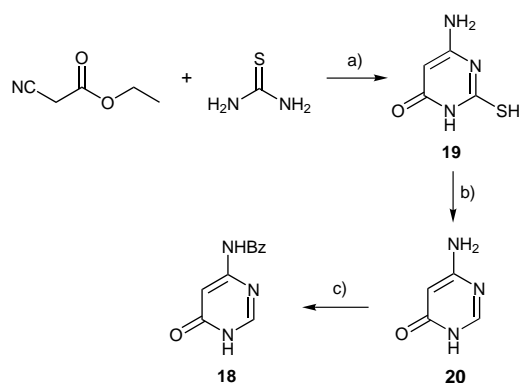
Fmoc protection of the primary aliphatic amino group in **7** and **8–10** was crucial for the success of the synthesis depicted in Scheme 1. This protecting group is stable under the acidic conditions required to remove the isopropylidene and methoxy protecting groups in starting material **6** and subsequent intermediates in the synthesis. Also, it is stable under the conditions of the nucleosidation reaction and could be



Scheme 2. Synthesis of the activated catechol ester **11** and conversion into comparison compound **5**. a) HNO₃/H₂SO₄, CH₂Cl₂, 94%. b) 48% aq. HBr, 79%. c) HOSu, DCC, THF, 53%. d) MeO(CH₂)₂NH₂, NEt₃, DMF, 75%.



Scheme 3. Synthesis of the nucleosidation precursor **7**. a) NaH, Cl(CH₂)₂NH₂·HCl, DMF, 88%. b) FmocOSu, NEt₃, DMF, 65%. c) Aq. HOAc, 96%. d) Ac₂O, pyridine, 83%.



Scheme 4. Synthesis of 6-benzoylamino-3,4-dihydropyrimidin-4-one (**18**). a) EtONa, EtOH, 93%. b) Ra-Ni, aq. NH₃, 47%. c) Benzoic anhydride, 83%.

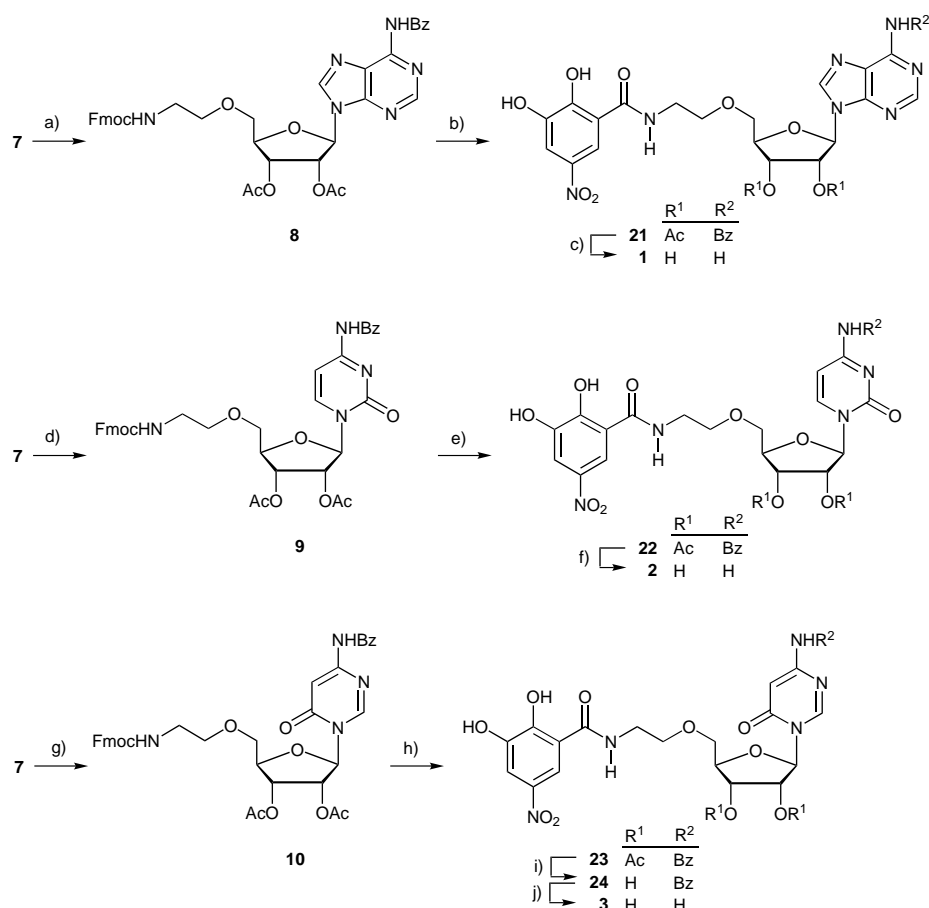
selectively removed under mild basic conditions in the presence of the acetyl protecting groups on the ribose and the *N*-benzoyl base protecting groups in **8–10**. Other *N*-protecting groups such as the trifluoroacetyl and the Cbz (benzyloxycarbonyl) groups, which were tested in the synthesis, did not satisfy these requirements.

In the successful synthesis of the bisubstrate inhibitors **1–3**, ribose derivative **6** was alkylated with 2-chloroethylamine to give **15** in 88% yield (Scheme 3). Protection with Fmoc-*O*-succinimide ester (FmocOSu)^[34] yielded **16** (65%). The reaction conditions were optimized to avoid formation of a byproduct arising from Fmoc deprotection of **16** by unreacted amine **15**. Treatment with aqueous HOAc effected cleavage of the isopropylidene and methoxy groups, affording ribose **17** in 96% yield. Subsequent peracetylation provided the acetylated derivative **7** (83%).

The syntheses of *N*-benzoylated adenine and cytosine for the subsequent nucleosidation reaction have been reported,^[35]

whereas 6-benzoylamino-3,4-dihydropyrimidin-4-one (**18**) was obtained in three steps by reacting thiourea and ethyl cyanoacetate in the presence of base to give **19**,^[36] desulfurization with Raney-Ni to **20**,^[37] and benzoylation (Scheme 4).

For the one-step nucleosidation of **7**, the *N*-benzoylated bases were silylated in situ using *N,O*-bis(trimethylsilyl)acetamide (BSA), yielding in all cases exclusively the β -anomer, according to the neighboring group participation of the α -acetoxy group at C(2'). The best results were obtained with trimethylsilyl triflate (TMSOTf) as Lewis acid which gave the nucleosides **9** and **10** in 79% and 58% yield, respectively (Scheme 5). However, the use of TMSOTf in the nucleosidation with *N*-benzoylated adenine led to the exclusive formation of the wrong regioisomer with bond formation occurring between N(7) of adenine and C(1') of the ribose. In contrast, the use of SnCl₄ as Lewis acid led to the desired nucleosidation product **8** in 65% yield, although some side reactions of SnCl₄ with the Fmoc group in **7** occurred. The use of SnCl₄ in the nucleosidation with **18** gave rise to a dimeric byproduct where nucleosidation occurred on the Fmoc-protected

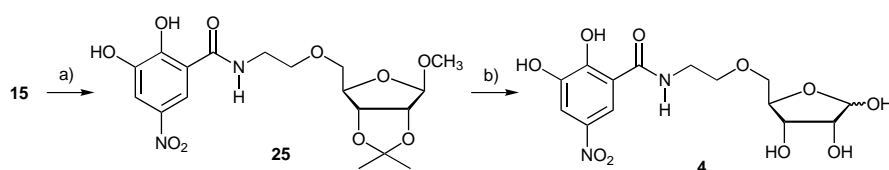


Scheme 5. Synthesis of the potential bisubstrate inhibitors **1–3**. a) *N*-Benzoyladenine, BSA, SnCl₄, MeCN, 65%. b) HNEt₂, DMF, then **11**, NEt₃, DMF, 30%. c) MeNH₂, EtOH, 82%. d) *N*-Benzoylcytosine, BSA, TMSOTf, MeCN, 79%. e) HNEt₂, DMF, then **11**, NEt₃, DMF, 49%. f) MeNH₂, EtOH, 82%. g) **18**, BSA, TMSOTf, MeCN, 58%. h) HNEt₂, DMF, then **11**, NEt₃, DMF, 56%. i) MeNH₂, EtOH, 80%. j) NH₃, MeOH/H₂O, 82%.

N-atom in **7** and on C(1') of the ribose. Constitution and configuration of the products were confirmed by NOE difference spectroscopy and {H,H}- and {H,C}-COSY 2D NMR experiments. Fmoc deprotection of **8–10** and coupling with the activated catechol ester **11** were performed in one step (Scheme 5). When piperidine or HNMe₂ (0.5–20%) in DMF/H₂O were used at varying temperatures in the removal of the Fmoc group, intermolecular deacylation of the formed free amines occurred readily. The deprotection step was, however, done successfully without deacylation of the ribose under high dilution conditions in DMF/HNEt₂ 1:1. The base HNEt₂ was readily removed by evaporation at reduced pressure leading to a solution of the free amine in DMF, which was directly used in the coupling to catechol **11**, affording **21–23** in yields of 30, 49, and 56%, respectively.

The synthesis of the target compounds **1–3** was completed by full deprotection. Starting from **21** or **22**, a one-step deprotection using MeNH₂ in EtOH for 20 min at 20 °C afforded **1** or **2**, respectively, in 82% yield. The same reaction conditions led only to cleavage of the acetate groups in **23** to give compound **24** (80%). However, compounds **24** or **23** could be transformed into **3** in 82% yield using 25% aq. NH₃/MeOH 1:1 for 18 h at 55 °C.

For the preparation of the compound **4**, ribose **15** was coupled to **11** to give **25** (75%), which was deprotected with aq. H₂SO₄ (91%) (Scheme 6).



Scheme 6. Synthesis of compound **4**. a) NEt₃, DMF, 75%. b) H₂SO₄, 91%.

Biological results: The compounds synthesized were tested for in vitro inhibitory activity with COMT obtained from rat liver. The IC₅₀ values (concentration of inhibitor at which 50% activity of the enzyme is observed) determined in the radiochemical assay developed by Zürcher et al.^[38] are listed in Table 1. In the case of the potential bisubstrate inhibitors, the assays were performed with and without preincubation of the enzyme with the inhibitor in the absence of both

Table 1. IC₅₀ values of potential bisubstrate inhibitors **1–3**, precursors **21–24**, and model compounds **4**, **25**, and **5** determined with and without preincubation in the presence of inhibitor. Preincubation was performed in the absence of both benzene-1,2-diol and SAM.

Compound	IC ₅₀ [μM] with preincubation	IC ₅₀ [μM] without preincubation
1	2	4
2	–	522
3	–	> 100
4	35	27
5	25	26
21	–	100
22	193	147
23	28	24
24	255	231
25	26	25

substrates (benzene-1,2-diol, SAM). For some inhibitors, the mechanism of binding to the enzyme was found to be different with and without preincubation.^[39, 40] In the assay, the substrate benzene-1,2-diol, the cofactor, and varying concentrations of inhibitor are incubated with the enzyme in a buffered aqueous solution containing Mg²⁺ ions. The cofactor SAM carries a tritiated methyl group, which is transferred to the substrate upon incubation with the enzyme. The product (³H)-2-methoxyphenol is extracted into the organic phase, whereas (³H)-SAM remains in the aqueous phase. The product concentration is measured by counting the decays per min (dpm) in the organic phase.

The results show that molecule **1** is a ten-fold more potent inhibitor than catechol **5**. This could be the result of its bisubstrate nature, which enables it to occupy both the catechol and SAM binding sites. The nearly identical IC₅₀ values with (2 μM) and without preincubation (4 μM) support similar inhibition modes in the two assays. Compounds **25** and **4** have an inhibitory activity in the same range as catechol **5**. This indicates that addition of a ribose fragment alone does not improve the inhibitory effect of the catechol moiety. The potential bisubstrate inhibitors **2** and **3** did not exhibit a significant inhibitory activity.

To investigate the mechanism of enzyme inhibition by molecule **1**, kinetic studies were performed. To determine the inhibition mode with respect to the catechol pocket, the concentration of benzene-1,2-diol was varied at saturated SAM concentration for different inhibitor concentrations. Assays were performed with and without 15 min of preincubation of the enzyme in the presence of inhibitor. The incubation time was 1 min.

The mechanism of an inhibitor binding to an enzyme in the presence of the substrate is elucidated by application of the Michaelis–Menten equation to determine whether the experimental data is in accordance with a distinct inhibitory mechanism. If the Michaelis–Menten equation applies, the inhibitory mechanism could be competitive, noncompetitive, or uncompetitive. A graphical procedure for data analysis is the Lineweaver–Burk plot which is the graph of 1/*v* (reaction rate) against 1/*s* (substrate concentration) at varying inhibitor concentrations. These plots should give straight lines. If the lines intersect at the same point on the ordinate, the inhibitory mechanism is said to be competitive. If they intersect at the same point on the abscissa, it is noncompetitive. Parallel lines indicate an uncompetitive mechanism. An error analysis was performed on the data of the radioactivity measurements (decays per min) and a weighted linear regression applied (Levenberg–Marquardt algorithm) to generate the Lineweaver–Burk plots. Lineweaver–Burk plots and plots of 1/*v* against *i* (inhibitor concentration) were used to process the data and to calculate the values for *K_M* (benzene-1,2-diol) = 357 ± 30 μM, *K_M*(SAM) = 33 ± 5 μM, and *K_i*^[41] (Table 2) (*K_M* = concentration of substrate at which the reaction rate *v* is half that of the maximum value; *K_i* = concentration of inhibitor at which the *K_M* value of the enzyme for the

Table 2. K_i values and inhibition mechanisms of the bisubstrate inhibitor **1** and the model compound **5** with respect to both benzene-1,2-diol and SAM.^[41]

Inhibitor	Inhibition mechanism with regard to benzene-1,2-diol	Inhibition mechanism with regard to SAM	K_i [μM] with regard to benzene-1,2-diol	K_i [μM] with regard to SAM
1	noncompetitive	competitive	0.55 ± 0.1	0.3 ± 0.1
5	competitive	uncompetitive		
23		uncompetitive		

corresponding substrate is doubled). The two K_M values are in good agreement with literature results.^[38, 39]

Inhibitor **1** shows a noncompetitive inhibitory mechanism with respect to the catechol binding site (Figure 4) with and without preincubation. For comparison, the same studies were performed on catechol **5**. It shows a competitive inhibition pattern as would be expected for a derivative of benzene-1,2-diol (data not shown).

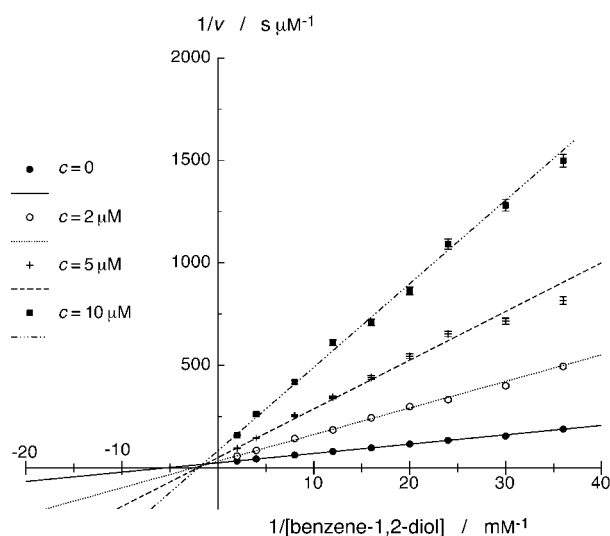


Figure 4. Lineweaver–Burk plot of reciprocal enzymatic activity vs. reciprocal benzene-1,2-diol concentration for varying concentrations of inhibitor **1** at saturating SAM concentration.

To determine the inhibition mechanism with respect to the SAM binding site, the concentration of SAM was varied at saturated benzene-1,2-diol concentration for different concentrations of inhibitor. The Lineweaver–Burk plot for inhibitor **1** (Figure 5) reveals a competitive inhibition pattern with and without preincubation. Model compound **5** features an uncompetitive inhibition mechanism under the same conditions, which is expected for a compound that does not bind to the SAM binding site (data not shown).^[39] This can be understood considering that SAM binds to the enzyme– Mg^{2+} complex prior to the substrate.

The potential bisubstrate inhibitor **23** was also studied for its kinetic behavior with respect to the SAM binding site. It showed an uncompetitive mechanism which implies that it does not bind to this site (data not shown).

When a preparation of the bisubstrate inhibitor **1** preincubated with the enzyme was dialyzed, the inhibition decreased by 50% within 5 h. This indicates that the inhibitor binds reversibly but its dissociation from the enzyme is rather slow and in the same range as that of tight binding inhibitors of COMT.^[39]

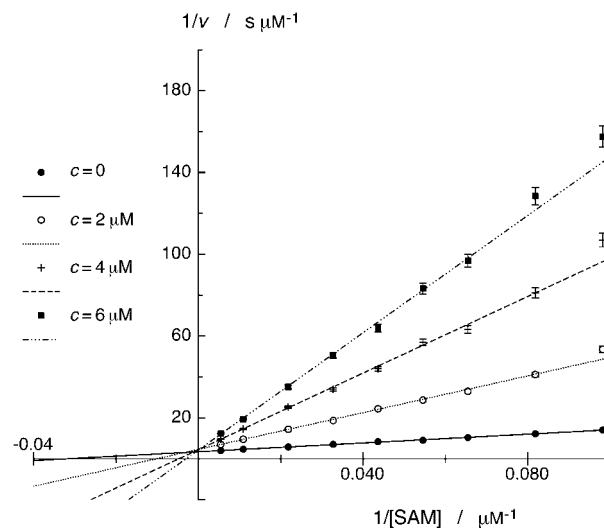


Figure 5. Lineweaver–Burk plot of reciprocal enzymatic activity vs. reciprocal SAM concentration for varying concentrations of inhibitor **1** at saturating benzene-1,2-diol concentration.

Discussion and Conclusion

It is known that binding of the cofactor SAM to the COMT– Mg^{2+} complex occurs prior to the binding of the catechol substrate.^[3] Complexation of SAM actually induces the formation of the catechol binding site as can be seen by comparison of the X-ray crystal structure of the apoenzyme^[20] with the structure of the quaternary complex containing SAM and 3,5-dinitrocatechol.^[20, 21] The catechol substrate does not bind to the enzyme without prior complexation of SAM. Analogues of SAM, which were tested as inhibitors of COMT, exhibit a competitive inhibition mechanism for the SAM binding site.^[10–12] For compound **1**, a competitive inhibition mechanism with regard to the SAM binding site was also found, which would be expected for a bisubstrate inhibitor.

The binding of inhibitors to the catechol binding site has been thoroughly studied for many catechols.^[39, 42] Mostly, catechols which inhibit the enzyme in the micromolar concentration range exhibit a competitive inhibition mechanism such as model compound **5**, whereas inhibitors with a high affinity to COMT such as tolcapone^[6] ($\text{IC}_{50} = 40 \text{ nM}$) and entacapone ($\text{IC}_{50} = 160 \text{ nM}$)^[8] typically bind in a noncompetitive fashion to the enzyme after preincubation with the enzyme^[40] and in a competitive mechanism without preincubation.

For compound **1**, a noncompetitive inhibition mechanism was found with respect to the catechol binding site. Because model compound **5** does bind to the catechol binding site in a competitive mechanism, it is not likely that the catechol

residue in the bisubstrate inhibitor **1** binds to a different site in the enzyme. Based on the order of binding of the natural substrates, two interpretations of the observed kinetics are possible. Binding of the bisubstrate inhibitor to the SAM binding pocket induces alterations in the binding characteristics of the catechol site compared to when SAM is bound. This leads to a noncompetitive mechanism for the binding of the bisubstrate inhibitor **1** to the catechol binding site. Alternatively, the bisubstrate nature of the inhibitor influences the affinity of its catechol residue for the catechol binding site. This could result in a situation where the catechol residue of the inhibitor **1** is “locked” into the binding site, which might resemble the noncompetitive kinetics found for tight binding inhibitors after preincubation.^[40] The latter hypothesis is supported by the slow dissociation of the inhibitor from the enzyme as observed in the dialysis experiments. In both cases, the bisubstrate inhibitor must dock into the SAM binding site before it binds to the catechol binding pocket (Figure 6). A co-crystallization of the bisubstrate inhibitor **1** and COMT is currently undertaken to further clarify the exact complexation mode.

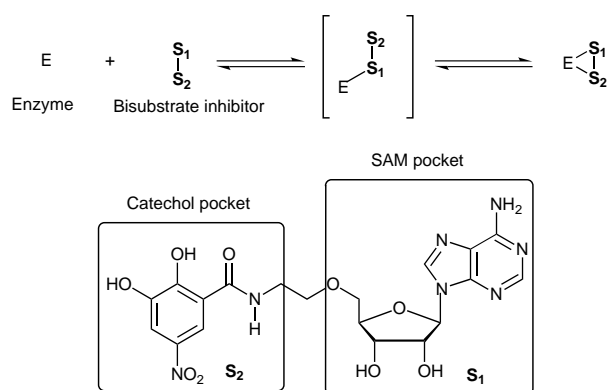


Figure 6. Summary of the kinetic results: Bisubstrate inhibitor **1** binds to the SAM pocket prior to binding to the catechol pocket in COMT.

The biological studies reveal strong structure–activity relationships for the binding of bisubstrate inhibitors to COMT. The precursor of compound **1**, compound **21**, is 50 times less active. The two other compounds designed as potential bisubstrate inhibitors, **2** and **3**, and their precursors **22–24** are less active than compound **1** by orders of magnitude and they are not bisubstrate inhibitors. Although **2** and **3** contain the same catechol motif as model compounds **4**, **5**, and **25**, they are much less potent inhibitors. Apparently, their catechol moiety can not bind efficiently to the catechol pocket presumably due to steric interactions between the bulky rest of these molecules and the amino acids lining this pocket. This provides further support to the hypothesis that a bisubstrate inhibitor such as **1** first occupies the SAM binding site and, in a second step, the catechol pocket. The comparison between **1**, **2**, and **3** demonstrates that the appropriate choice of adenine substitutes is crucial for biological activity of compounds designed as bisubstrate inhibitors. It can be speculated that the bridge connecting the nucleoside and catechol moieties is only of suitable length in **1** but not in **2**

and **3** with their smaller bases, although the modeling studies do not provide conclusive support for such an assumption. Finally, the hypothesis that the “methionine-binding channel” can be neglected in the design of potent bisubstrate inhibitors for COMT was confirmed in clear way.

We are now targeting the next generations of bisubstrate inhibitors for COMT, focusing on different adenine substitutions, the introduction of connectors of different size and shape between nucleobase and catechol moieties, as well as the substitution of the ribose moiety.

Experimental Section

General methods: Reagents and solvents were purchased reagent-grade and used without further purification. Solvents (DMF, pyridine, MeCN) were dried for 12 h over molecular sieves (4 Å). *N*-Benzoyladenine and *N*-benzoylcytosine were prepared as described [35]. Evaporation and concentration in vacuo was performed at water aspirator pressure. Drying under vacuum was done at 0.05 Torr. Thin-layer chromatography was performed on glass-backed sheets coated with either SiO₂ 60 F₂₅₄ or neutral Al₂O₃ from Merck, containing fluorescent indicator UV₂₅₄. Column chromatography (CC) was performed using Fluka SiO₂ 60, 40–63 mesh, or Fluka SiO₂H, 5–40 mesh. Flash column chromatography (FC) was performed at a pressure of 0.0–0.4 bar (SiO₂ 60) and of 1 bar (SiO₂H). Analytical HPLC was performed with a Knauer HPLC system with WellChrom Maxi-Star K-1000 pumps with a flow of 1 mL min⁻¹ using a Nucleosil RP18 (240 mm 4 mm, 100 Å/5) column from Macherey–Nagel and UV detection (220 nm, 254 nm). Melting points were determined on a Büchi SMP-20 apparatus and are uncorrected. Optical rotations were measured on a Perkin–Elmer 241 polarimeter at λ = 589 nm. Infrared spectra were recorded on a Perkin–Elmer 1600-FT-IR spectrometer. ¹H and ¹³C NMR spectra were recorded on Varian Gemini-200 and -300 and Bruker AMX-500 spectrometers. FAB mass spectra were recorded on a VG-ZAB-2SEQ instrument using 3-nitrobenzyl alcohol as a matrix. A VG Tribid instrument was used for EI and a Finnigan MAT TSO 7000 instrument for electrospray ionization (ESI) mass spectrometry. Elemental analyses were made by the Mikrolabor in the Laboratorium für Organische Chemie at ETH Zürich.

2-Hydroxy-3-methoxy-5-nitrobenzoic acid (13):^[43] A mixture of H₂SO₄ (98 %, 3.27 mL) and HNO₃ (68 %, 2.73 mL) was added over 15 min at 0 °C with stirring to **12** (5.00 g, 29.73 mmol) in CH₂Cl₂ (33 mL). The solution was stirred for 1 h at 0 °C, warmed to 20 °C, and stirred for another 2 h. The mixture was poured into ice water (50 mL), and the white precipitate was filtered off, washed (H₂O), and dried in vacuo at 40 °C for 14 h to give **13** (5.95 g, 94 %). M.p. 220 °C; IR (KBr): $\tilde{\nu}$ = 3108, 1667, 1526, 1455, 1336, 1262, 1170, 1095, 1060, 867, 774, 741, 696, 478 cm⁻¹; ¹H NMR (200 MHz, CD₃OD): δ = 8.38 (d, *J* = 2.5 Hz, 1H), 7.94 (d, *J* = 2.5 Hz, 1H), 3.97 (s, 3H); ¹³C NMR (50 MHz, CD₃OD): δ = 171.12, 157.56, 148.96, 139.25, 117.63, 109.99, 109.89, 55.61; MS (EI): *m/z* (%): 213 (41) [*M*]⁺, 195 (100) [*M* – H₂O]⁺; HR-MS (EI): calcd for C₈H₇NO₆⁺ [*M*]⁺: 213.0273; found: 213.0268.

2,3-Dihydroxy-5-nitrobenzoic acid (14):^[33] A solution of **13** (7.30 g, 34.28 mmol) in HBr (48 % in H₂O, 200 mL) was heated for 4 h at 135 °C. The volatiles were removed by distillation (0.02 Torr). The remaining dark solid was redissolved twice in a mixture of toluene (100 mL) and H₂O (100 mL) and distilled again to remove residual HBr. The solid residue was purified by recrystallization from toluene and sublimed to yield **14** as a light yellow solid (5.40 g, 79 %). M.p. 222 °C; IR (KBr): $\tilde{\nu}$ = 3511, 3400, 3096, 2844, 2567, 1672, 1526, 1470, 1345, 1278, 1223, 1156, 1081, 985, 900, 798, 769, 743, 696, 489 cm⁻¹; ¹H NMR (200 MHz, CD₃OD): δ = 8.28 (d, *J* = 3.0 Hz, 1H), 7.81 (d, *J* = 3.0 Hz, 1H); ¹³C NMR (50 MHz, CD₃OD): δ = 171.34, 156.17, 146.74, 139.44, 116.49, 113.67, 112.2; MS (EI): *m/z* (%): 199 (29) [*M*]⁺, 181 (100) [*M* – H₂O]⁺; C₇H₅NO₆ · 0.5 H₂O (208.13): calcd: C 40.40, H 2.91, N 6.71; found: C 40.52, H 2.80, N 6.51.

2,5-Dioxotetrahydro-1H-pyrrol-1-yl 2,3-dihydroxy-5-nitrobenzoate (11): *N*-Hydroxysuccinimide (173 mg, 1.51 mmol) and DCC (312 mg, 1.51 mmol) were added at 0 °C to **14** (300 mg, 1.51 mmol) in THF (3 mL).

The mixture was stirred for 1 h at 0 °C during which time a white precipitate formed. The suspension was left in the refrigerator at 4 °C overnight, then the white precipitate was filtered off and washed with THF (5 mL). Evaporation of the filtrate in vacuo and recrystallization from 2-propanol gave **11** as cream-colored needles (232 mg, 53%). M.p. 209 °C; IR (KBr): $\tilde{\nu}$ = 3402, 1736, 1542, 1473, 1346, 1306, 1200, 1111, 1072, 972, 922, 783, 739, 650, 606 cm⁻¹; ¹H NMR (200 MHz, [D₆]DMSO): δ = 8.18 (d, *J* = 2.8 Hz, 1 H), 7.85 (d, *J* = 2.8 Hz, 1 H), 2.90 (s, 4 H); ¹³C NMR (125 MHz, CD₃OD): δ = 171.59, 162.79, 156.69, 148.62, 140.96, 118.32, 115.13, 111.10, 26.60; MS (EI): *m/z*: 296 [M]⁺; C₁₁H₈N₂O₈ (296.19): calcd: C 44.61, H 2.72, N 9.46; found: C 44.48, H 2.90, N 9.23.

N-(2-Methoxyethyl)-2,3-dihydroxy-5-nitrobenzamide (5): 2-Methoxyethylamine (92 μ L, 1.06 mmol) and NEt₃ (0.18 mL, 1.29 mmol) were added to **11** (0.15 g, 0.50 mmol) in DMF (1 mL), and the mixture was stirred for 4 h at 20 °C. Evaporation in vacuo and FC (SiO₂, CH₂Cl₂/acetone/HCOOH 80:19:1) gave **5** (97 mg, 75%) as a yellow powder. M.p. 143 °C; IR (KBr): $\tilde{\nu}$ = 3389, 3089, 2933, 2833, 1644, 1606, 1556, 1511, 1472, 1339, 1172, 1100, 1011, 944, 900, 833, 783, 744, 711, 661, 583, 450 cm⁻¹; ¹H NMR (200 MHz, CDCl₃): δ = 8.03 (d, *J* = 2.4 Hz, 1 H), 7.92 (d, *J* = 2.4 Hz, 1 H), 6.94 (s, 1 H), 6.06 (s, 1 H), 3.72–3.62 (m, 4 H), 3.46 (s, 3 H); ¹³C NMR (75 MHz, CD₃OD): δ = 170.03, 157.22, 148.60, 140.70, 116.52, 116.44, 113.22, 71.95, 59.15, 40.55; MS (EI): *m/z* (%): 256 (56) [M]⁺, 182 (100) [M – MeO(CH₂)₂NH]⁺; C₁₀H₁₂N₂O₆ (256.21): calcd: C 46.87, H 4.72, N 10.93; found: C 46.92, H 4.73, N 10.71.

2-[(3*aR*,4*R*,6*R*,6*aR*)-6-Methoxy-2,2-dimethylperhydrofuro[3,4-*d*][1,3]dioxol-4-yl)methoxy]ethylamine (15): Sodium hydride (55–65% dispersion in mineral oil, 12.00 g, 250.00 mmol) was added over 1 h to a solution of **6** (4.99 g, 24.41 mmol) in DMF (150 mL) at 0 °C under Ar. The mixture was stirred for 1 h at 20 °C, then 2-chlorethylamine hydrochloride (17.40 g, 150 mmol) was added over 1 h at –5 to 0 °C. After stirring for 5 h at 20 °C, MeOH (100 mL) was added, the solvents were evaporated in vacuo, and CC (SiO₂, CH₂Cl₂/MeOH/NEt₃ 90:10:5) provided **15** as a colorless oil (5.32 g, 88%). [α]_D²⁰ = –63.0 (*c* = 1.0, CHCl₃); IR (CHCl₃): $\tilde{\nu}$ = 3377, 3200, 2938, 1681, 1584, 1456, 1383, 1267, 1238, 1160, 1110, 1014, 962, 869, 660 cm⁻¹; ¹H NMR (200 MHz, CDCl₃): δ = 4.99 (s, 1 H), 4.71 (d, *J* = 6.2 Hz, 1 H), 4.61 (d, *J* = 6.2 Hz, 1 H), 4.36–4.33 (m, 1 H), 3.58–3.47 (m, 4 H), 3.36 (s, 3 H), 2.90 (t, *J* = 5.4 Hz, 2 H), 1.52 (s, 3 H), 1.36 (s, 3 H); ¹³C NMR (50 MHz, CDCl₃): δ = 110.05, 106.97, 82.81, 82.71, 79.73, 71.04, 69.54, 52.37, 39.36, 24.00, 22.54; HR-MS (EI): calcd for C₁₁H₂₂NO₅⁺ [MH]⁺: 248.1498; found: 248.1503.

9*H*-Fluoren-9-ylmethyl N-[2-[(3*aR*,4*R*,6*R*,6*aR*)-6-methoxy-2,2-dimethylperhydrofuro[3,4-*d*][1,3]dioxol-4-yl)methoxy]ethyl]carbamate (16): NEt₃ (1.8 mL, 12.12 mmol) and FmocOSu (4.35 g, 12.12 mmol) were added under stirring at 0 °C to **15** (1.00 g, 4.04 mmol) in DMF (50 mL). After 10 min, H₂O (50 mL) was added and the mixture was extracted with CH₂Cl₂ (3 \times 100 mL). The combined organic phases were washed with H₂O (4 \times 100 mL) and dried (MgSO₄). Evaporation in vacuo and FC (SiO₂, hexane/EtOAc 3:2) afforded **16** as a white powder (1.23 g, 65%). M.p. 94–95 °C; [α]_D²⁰ = –41.0 (*c* = 1.0, CHCl₃); IR (neat): $\tilde{\nu}$ = 3442, 3027, 1715, 1515, 1231, 1110, 803 cm⁻¹; ¹H NMR (300 MHz, CDCl₃): δ = 7.78 (d, *J* = 7.5 Hz, 2 H), 7.62 (d, *J* = 7.5 Hz, 2 H), 7.43–7.29 (m, 4 H), 5.48 (brs, 1 H), 4.98 (s, 1 H), 4.70 (d, *J* = 6.3 Hz, 1 H), 4.60 (d, *J* = 6.3 Hz, 1 H), 4.42 (d, *J* = 6.9 Hz, 2 H), 4.35 (t, *J* = 6.0 Hz, 1 H), 4.22 (t, *J* = 6.9 Hz, 1 H), 3.57–3.40 (m, 6 H), 3.31 (s, 3 H), 1.50 (s, 3 H), 1.33 (s, 3 H); ¹³C NMR (50 MHz, CDCl₃): δ = 154.26, 141.72, 139.03, 125.35, 124.71, 122.74, 117.63, 110.08, 107.6, 83.07, 82.81, 79.61, 69.70, 67.35, 64.24, 52.56, 44.85, 38.50, 24.06, 22.57; MS (FAB): *m/z*: 470 [M]⁺; C₂₆H₃₁N₃O₇ (469.53): calcd: C 66.51, H 6.65, N 2.98; found: C 66.58, H 6.75, N 2.91.

9*H*-Fluoren-9-ylmethyl N-[2-[(2*R*,3*R*,4*R*)-3,4,5-trihydroxytetrahydrofuran-2-yl)methoxy]ethyl]carbamate (17): A solution of **16** (1.50 g, 3.19 mmol) in HOAc (70% in H₂O, 100 mL) was heated for 5 h at 90 °C, then the mixture was evaporated in vacuo. Toluene was added twice followed each time by evaporation in vacuo, yielding **17** as a white solid which was used without further purification (1.27 g, 96%). M.p. 118–120 °C; IR (KBr): $\tilde{\nu}$ = 3323, 3056, 2933, 1690, 1543, 1444, 1265, 1120, 1017, 739 cm⁻¹; ¹H NMR (200 MHz, CDCl₃, mixture of anomers): δ = 7.79 (d, *J* = 8.0 Hz, 2 H), 7.62 (d, *J* = 8.0 Hz, 2 H), 7.45–7.17 (m, 4 H), 5.50–5.20 (m, 2 H), 4.43 (d, *J* = 6.0 Hz, 2 H), 4.30–3.90 (m, 4 H), 3.70–3.20 (m, 6 H); ¹³C NMR (75 MHz, CDCl₃, mixture of anomers): δ = 157.09, 144.18, 141.58, 141.48, 127.97, 127.34, 127.23, 125.29, 120.24, 108.75, 102.26, 96.76, 82.20,

81.86, 71.70, 70.72, 70.09, 67.30, 66.84, 47.26, 41.50, 40.79; HR-MS (FAB): calcd for C₂₅H₂₆NO₇⁺ [MH]⁺: 416.1702; found: 416.1702.

(3*R*,4*R*,5*R*)-5-[2-[(9*H*-Fluoren-9-ylmethoxy)carbonyl]amino]ethoxy-methyl]tetrahydrofuran-2,3,4-triyl triacetate (7): Ac₂O (2.40 mL, 25.40 mmol) was added to **17** (1.20 g, 2.89 mmol) in pyridine (4 mL), and the mixture was stirred for 24 h at 20 °C. After addition of a saturated aqueous solution of NaHCO₃ (20 mL), the mixture was extracted three times with EtOAc (50 mL) and the combined organic phases were dried (MgSO₄) and evaporated in vacuo. FC (SiO₂, hexane/EtOAc 1:1) gave **7** as a white powder (1.3 g, 83%). M.p. 65 °C; IR (KBr): $\tilde{\nu}$ = 3400, 2933, 1750, 1528, 1450, 1367, 1222, 1106, 1022, 961, 894, 739 cm⁻¹; ¹H NMR (200 MHz, CDCl₃, mixture of anomers): δ = 7.80 (d, *J* = 8.0 Hz, 2 H), 7.66 (d, *J* = 8.0 Hz, 2 H), 7.36–7.27 (m, 4 H), 6.19 (s, 1 H), 5.55–5.35 (m, 3 H), 4.50–4.20 (m, 4 H), 3.75–3.30 (m, 6 H), 2.14, 2.11, 2.10, 2.09, 2.07 (5s, 9 H); ¹³C NMR (75 MHz, CDCl₃, mixture of anomers): δ = 170.35, 169.92, 169.54, 169.16, 156.63, 143.98, 141.31, 127.81, 127.73, 127.68, 127.58, 127.19, 126.93, 125.20, 125.07, 120.00, 199.96, 98.33, 98.30, 81.17, 80.84, 74.50, 74.21, 70.90, 70.65, 47.33, 47.17, 40.72, 20.22, 20.56, 21.07, 21.25, 21.51, 21.73; MS (FAB): *m/z* (%): 482 (100) [M – OAc]⁺; C₂₈H₃₁NO₁₀ (540.55): calcd: C 62.22, H 5.59, N 2.59, O 29.60; found: C 62.01, H 5.80, N 2.53, O 29.83.

6-Amino-2-sulfanyl-3,4-dihydropyrimidin-4-one (19):^[6] Thiourea (4.56 g, 60.00 mmol) and ethyl cyanoacetate (6.40 mL, 60.00 mmol) were added to EtONa (4.29 g, 63.00 mmol) in EtOH (44 mL), and the mixture was heated to reflux for 2 h. The formed precipitate was filtered off, and the solvents were evaporated in vacuo. The resulting solid residue and the initial precipitate were dissolved in H₂O (50 mL), then HOAc was added until complete precipitation of **19** as a white powder (8.00 g, 93%). M.p. 295 °C; IR (KBr): $\tilde{\nu}$ = 3322, 1556, 1298, 1187, 1000, 922, 833, 790, 613, 574, 525 cm⁻¹; ¹H NMR (300 MHz, [D₆]DMSO): δ = 11.55 (s, 1 H), 6.38 (s, 2 H), 4.69 (s, 1 H); HR-MS (FAB): calcd for C₄H₆N₃O⁺ [MH]⁺: 144.0232; found: 144.0231.

6-Amino-3,4-dihydropyrimidin-4-one (20):^[37] An aqueous suspension of Ra-Ni (12.00 g) was added to a vigorously stirred mixture of **19** (3.00 g, 20.96 mmol) in H₂O (30 mL) and NH₃ (25% in H₂O, 1.82 mL) at reflux. After 1 h, the Ra-Ni was filtered off and washed with boiling H₂O. Evaporation and recrystallization (H₂O) yielded **20** (1.10 g, 47%) as a white powder. M.p. 263–264 °C; IR (KBr): $\tilde{\nu}$ = 3322, 3142, 2922, 2767, 1939, 1661, 1614, 1544, 1495, 1447, 1367, 1305, 1242, 1200, 1094, 990, 914, 808, 767, 609, 565, 526, 449, 418 cm⁻¹; ¹H NMR (300 MHz, [D₆]DMSO): δ = 11.38 (s, 1 H), 7.74 (s, 1 H), 6.38 (s, 2 H), 4.94 (s, 1 H); MS (FAB): *m/z* (%): 111.9 (100) [MH]⁺; HR-MS (FAB): calcd for C₄H₆N₃O⁺ [MH]⁺: 112.0511; found: 112.0506; C₄H₆ON₃ (111.10): calcd: C 43.24, H 4.54, N 37.82; found: C 43.42, H 4.73, N 37.85.

N-(6-Oxo-1,6-dihydropyrimidin-4-yl)benzamide (18). A mixture of **20** (0.61 g, 5.47 mmol) and benzoic anhydride (2.96 g, 13.08 mmol) was heated to 140 °C. After 2 h, EtOH (18 mL) was added at 90 °C and stirring was continued for 1 h. After the mixture was allowed to stand at 20 °C for 4 h, **18** (0.98 g, 83%) precipitated from the solution as a white powder. M.p. 275–276 °C; IR (KBr): $\tilde{\nu}$ = 3390, 3064, 1687, 1656, 1591, 1526, 1460, 1405, 1336, 1258, 1214, 1178, 985, 853, 720, 694, 636, 594, 516, 466 cm⁻¹; ¹H NMR (300 MHz, [D₆]DMSO): δ = 12.35 (s, 1 H), 10.69 (s, 1 H), 8.13 (s, 1 H), 8.00–7.80 (m, 2 H), 7.70–7.30 (m, 3 H), 7.05 (s, 1 H); ¹³C NMR (75 MHz, [D₆]DMSO): δ = 166.50, 162.50, 156.50, 149.50, 133.50, 131.90, 128.27, 128.04, 98.50; HR-MS (FAB): calcd for C₁₁H₁₀N₃O₂⁺ [MH]⁺: 216.0773; found: 216.0782.

(2*S*,3*R*,4*R*,5*R*)-2-[6-(Benzoylamino)purin-9-yl]-5-[2-[(9*H*-fluoren-9-ylmethoxy)carbonyl]amino]ethoxy)methyl]tetrahydrofuran-3,4-diyl diacetate (8): BSA (0.40 mL, 1.64 mmol) was added at 50 °C under Ar to a stirred suspension of 6-*N*-benzoyladenine (196 mg, 0.82 mmol) in MeCN (2 mL). After 10 min, a colorless solution formed to which **7** (0.37 g, 0.68 mmol) in MeCN (1 mL) and SnCl₄ (0.32 mL, 2.7 mmol) were added. Stirring was continued at 55 °C for 15 min, then saturated aqueous solution of NaHCO₃ (20 mL) and EtOAc (20 mL) were added and the mixture was extracted three times with EtOAc (50 mL). The organic phases were evaporated in vacuo, and FC (SiO₂, CH₂Cl₂/MeOH 99:1) provided **8** as a white powder (0.318 g, 65%). M.p. 100 °C; [α]_D²⁰ = –25.0 (*c* = 1.0, CHCl₃); IR (KBr): $\tilde{\nu}$ = 3420, 2922, 2367, 1750, 1717, 1694, 1611, 1578, 1517, 1450, 1372, 1244, 1094, 794, 761, 739, 711, 650, 567 cm⁻¹; ¹H NMR (500 MHz, CDCl₃): δ = 8.93 (s, 1 H), 8.81 (s, 1 H), 8.40 (s, 1 H), 7.91 (d, *J* = 7.5 Hz, 2 H), 7.69 (d, *J* = 7.5 Hz, 2 H), 7.59–7.55 (m, 3 H), 7.47–7.43 (m, 2 H), 7.33–7.18 (m, 4 H), 6.42 (d, *J* =

6.6 Hz, 1H), 6.03 (d, $J = 6.6$ Hz, 1H), 5.68–5.67 (m, 1H), 5.57 (t, $J = 5.4$ Hz, 1H), 4.41–4.40 (m, 1H), 4.37–4.35 (d, $J = 7.4$ Hz, 2H), 4.22 (t, $J = 7.4$ Hz, 1H), 3.85 (d, $J = 9.3$ Hz, 1H), 3.73 (d, $J = 5.2$ Hz, 2H), 3.62–3.61 (m, 1H), 3.50–3.48 (m, 2H), 2.17 (s, 3H), 2.07 (s, 3H); ^{13}C NMR (125 MHz, CDCl_3): $\delta = 167.63, 167.47, 162.26, 154.36, 150.68, 149.69, 147.34, 141.76, 141.69, 138.87, 131.15, 130.42, 126.49, 125.50, 125.28, 124.65, 124.55, 122.81, 117.57, 82.65, 80.08, 71.54, 69.42, 68.40, 67.96, 64.62, 44.69, 38.53, 18.22, 17.96$; MS (FAB): m/z (%): 743 (22) $[\text{M}+\text{Na}]^+$, 721 (100) $[\text{MH}]^+$; HR-MS (FAB): calcd for $\text{C}_{38}\text{H}_{37}\text{N}_6\text{O}_9^+$ $[\text{MH}]^+$: 721.2622; found: 721.2625.

(2S,3R,4R,5R)-2-[4-(Benzoylamino)-2-oxo-1,2-dihydropyrimidin-1-yl]-5-[2-[(9H-fluoren-9-ylmethoxy)carbonyl]amino]ethoxy)methyl]tetrahydrofuran-3,4-diyl diacetate (9): BSA (0.16 mL, 0.66 mmol) was added at 50 °C to a stirred suspension of 4-*N*-benzoylcytosine (72 mg, 0.33 mmol) in MeCN (2 mL). After 10 min, a colorless solution formed to which **7** (150 mg, 0.28 mmol) in MeCN (1 mL) and TMSOTf (0.25 mL, 1.38 mmol) were added under Ar. The mixture was stirred at 55 °C for 20 min, then quenched with a saturated aqueous solution of NaHCO_3 (20 mL) and EtOAc (20 mL), and extracted with EtOAc (3 \times 50 mL). The combined organic layers were evaporated in vacuo, and FC (SiO_2H , $\text{CH}_2\text{Cl}_2/\text{MeOH}$ 98.5:1.5) afforded **9** as a white powder (0.152 g, 79%). M.p. 184–185 °C; $[\alpha]_D^{20} = +29.0$ ($c = 1.0$, CHCl_3); IR (KBr): $\tilde{\nu} = 3370, 3067, 2956, 2878, 1746, 1695, 1670, 1615, 1555, 1525, 1488, 1374, 1309, 1248, 1139, 1090, 790, 738, 706\text{ cm}^{-1}$; ^1H NMR (500 MHz, CDCl_3): $\delta = 8.65$ (s, 1H), 8.21–8.18 (m, 1H), 7.78 (d, $J = 5.7$ Hz, 2H), 7.67 (d, $J = 7.5$ Hz, 2H), 7.65–7.55 (m, 4H), 7.48–7.44 (m, 2H), 7.36–7.32 (m, 2H), 7.28–7.22 (m, 2H), 6.37 (d, $J = 5.4$ Hz, 1H), 5.55–5.48 (m, 3H), 4.41 (d, $J = 7.3$ Hz, 2H), 4.33 (m, 1H), 4.23 (t, $J = 7.3$ Hz, 1H), 3.89 (d, $J = 10.4$ Hz, 1H), 3.77–3.75 (m, 1H), 3.68 (d, $J = 10.4$ Hz, 1H), 3.62–3.60 (m, 1H), 3.50–3.45 (m, 2H), 2.12 (s, 3H), 2.11 (s, 3H); ^{13}C NMR (125 MHz, CDCl_3): $\delta = 169.88, 166.04, 162.35, 156.58, 144.34, 144.01, 143.98, 141.21, 133.11, 128.91, 127.56, 126.94, 125.22, 125.19, 119.84, 87.44, 81.84, 74.22, 70.91, 70.71, 69.71, 66.94, 47.18, 40.97, 20.64, 20.51$ (3 peaks missing); MS (FAB): m/z (%): 697.2 (100) $[\text{MH}]^+$; HR-MS (FAB): calcd for $\text{C}_{37}\text{H}_{37}\text{N}_4\text{O}_{10}^+$ $[\text{MH}]^+$: 697.2509; found: 697.2516; $\text{C}_{37}\text{H}_{36}\text{N}_4\text{O}_{10}$ (696.72): calcd: C 63.79, H 5.21, N 7.76; found: C 63.85, H 5.39, N 7.97.

(2S,3R,4R,5R)-2-[4-(Benzoylamino)-6-oxo-1,6-dihydropyrimidin-1-yl]-5-[2-[(9H-fluoren-9-ylmethoxy)carbonyl]amino]ethoxy)methyl]tetrahydrofuran-3,4-diyl diacetate (10): BSA (0.38 mL, 1.55 mmol) was added under Ar at 60 °C to a stirred suspension of **18** (160 mg, 0.75 mmol) and **7** (168 mg, 0.31 mmol) in MeCN (2 mL), and the resulting colorless solution was stirred for 1 h at this temperature. TMSOTf (0.28 mL, 1.55 mmol) was added, and the mixture was stirred at 60 °C for 50 min, then saturated aqueous solutions of NaHCO_3 (20 mL) and EtOAc (20 mL) were added. The mixture was extracted with EtOAc (3 \times 50 mL), and the combined organic phases were evaporated in vacuo. FC (SiO_2H , $\text{CH}_2\text{Cl}_2/\text{MeOH}$ 100:1) afforded **10** as a white powder (0.11 g, 58%). M.p. 92 °C; $[\alpha]_D^{20} = +33.0$ ($c = 1.0$, CHCl_3); IR (KBr): $\tilde{\nu} = 3342, 3056, 938, 1750, 1961, 1508, 1444, 1372, 1329, 1243, 1094, 849, 760, 741\text{ cm}^{-1}$; ^1H NMR (300 MHz, CDCl_3): $\delta = 8.62$ (s, 1H), 7.97 (s, 1H), 7.70–7.16 (m, 14H), 6.34 (d, $J = 4.2$ Hz, 1H), 5.82–5.80 (m, 1H), 5.60–5.55 (m, 2H), 4.54–4.16 (m, 4H), 3.96–3.34 (m, 6H), 2.14 (s, 3H), 2.12 (s, 3H); ^{13}C NMR (125 MHz, CDCl_3): $\delta = 169.77, 169.57, 165.45, 161.44, 156.71, 154.01, 147.90, 143.89, 143.86, 141.28, 141.25, 133.14, 132.65, 128.98, 128.85, 127.70, 127.66, 127.18, 126.99, 126.95, 125.06, 124.95, 119.92, 98.24, 86.58, 81.68, 74.51, 70.83, 70.08, 69.20, 66.71, 47.25, 41.06, 20.60, 20.50$; MS (FAB): m/z (%): 719.2 (14) $[\text{M}+\text{Na}]^+$, 697.2 (100) $[\text{MH}]^+$; HR-MS (FAB): calcd for $\text{C}_{37}\text{H}_{37}\text{N}_4\text{O}_{10}$ $[\text{MH}]^+$: 697.2509; found: 697.2511.

(2S,3R,4R,5R)-2-[6-(Benzoylamino)purin-9-yl]-5-[(2,3-dihydroxy-5-nitrobenzoyl)amino]ethoxy)methyl]tetrahydrofuran-3,4-diyl diacetate (21): HNEt₂ (40 mL) was added to **8** (100 mg, 0.14 mmol) in DMF (40 mL), and the solution was stirred under Ar for 2.5 h at 20 °C. After evaporation of HNEt₂ in vacuo, **11** (41 mg, 0.14 mmol) and NEt₃ (0.06 mL, 0.43 mmol) were added and the mixture was stirred for 24 h at 20 °C. Evaporation in vacuo and recrystallization from 2-propanol gave **21** as an orange powder (28 mg, 30%). M.p. 127 °C; $[\alpha]_D^{20} = -21.0$ ($c = 1.0$, THF); IR (KBr): $\tilde{\nu} = 3411, 2922, 2344, 1744, 1700, 1639, 1611, 1583, 1516, 1460, 1336, 1241, 1073, 904, 792, 747, 708\text{ cm}^{-1}$; ^1H NMR (500 MHz, CDCl_3): $\delta = 8.71$ (s, 1H), 8.69 (s, 1H), 8.43 (d, $J = 2.7$ Hz, 1H), 8.06 (d, $J = 7.2$ Hz, 2H), 7.67–7.53 (m, 3H), 7.43 (d, $J = 2.7$ Hz, 1H), 6.37 (d, $J = 5.7$ Hz, 1H), 5.98 (t, $J = 5.7$ Hz, 1H), 5.81–5.78 (m, 1H), 4.29–4.28 (m, 1H), 3.94–3.59 (m, 6H), 2.15 (s, 3H), 2.00 (s, 3H); ^{13}C NMR (125 MHz, CD_3OD): $\delta = 170.09, 169.74, 168.52, 165.86, 152.33, 151.93, 151.53, 149.55, 146.74, 141.51, 133.22,$

132.61, 128.44, 127.89, 126.78, 122.53, 115.39, 113.88, 111.31, 85.45, 82.34, 73.15, 71.35, 69.81, 69.74, 39.09, 20.19, 19.87; HR-MS (FAB): calcd for $\text{C}_{30}\text{H}_{30}\text{N}_7\text{O}_{12}^+$ $[\text{MH}]^+$: 680.1952; found: 680.1952.

(2S,3R,4R,5R)-2-[4-(Benzoylamino)-2-oxo-1,2-dihydropyrimidin-1-yl]-5-[(2-[(2,3-dihydroxy-5-nitrobenzoyl)amino]ethoxy)methyl]tetrahydrofuran-3,4-diyl diacetate (22): Starting from **9** (100 mg, 0.14 mmol) and **11** (41 mg, 0.14 mmol), the procedure described for **21** afforded **22** (46 mg, 49%) as an orange powder. M.p. 146 °C; $[\alpha]_D^{20} = +40.0$ ($c = 1.0$, THF); IR (KBr): $\tilde{\nu} = 3422, 2978, 2933, 1750, 1700, 1656, 1628, 1561, 1483, 1372, 1311, 1250, 1128, 1072, 806, 783, 706\text{ cm}^{-1}$; ^1H NMR (500 MHz, CD_3OD): $\delta = 8.50$ (d, $J = 3.0$ Hz, 1H), 8.39 (d, $J = 7.6$ Hz, 1H), 8.00–7.90 (m, 2H), 7.67–7.56 (m, 3H), 7.51 (d, $J = 7.6$ Hz, 1H), 7.46 (d, $J = 3.0$ Hz, 1H), 6.24 (d, $J = 5.2$ Hz, 1H), 5.70–5.65 (m, 1H), 5.62–5.58 (m, 1H), 4.50–4.45 (m, 1H), 4.05–3.65 (m, 6H), 2.15 (s, 3H), 2.10 (s, 3H); ^{13}C NMR (125 MHz, CD_3OD): $\delta = 171.47, 171.14, 170.04, 168.81, 164.99, 157.96, 150.13, 146.07, 134.67, 134.00, 129.87, 129.74, 129.22, 120.53, 115.91, 108.17, 99.12, 96.76, 89.65, 83.92, 76.00, 72.75, 71.43, 70.73, 40.13, 20.53, 20.34$; MS (FAB): m/z (%): 678.1 (24) $[\text{M}+\text{Na}]^+$, 656.1 (100) $[\text{MH}]^+$; HR-MS (FAB): calcd for $\text{C}_{29}\text{H}_{29}\text{N}_5\text{O}_{13}^+$ $[\text{MH}]^+$: 656.1840; found: 656.1843.

(2S,3R,4R,5R)-2-[4-(Benzoylamino)-6-oxo-1,6-dihydropyrimidin-1-yl]-5-[(2-[(2,3-dihydroxy-5-nitrobenzoyl)amino]ethoxy)methyl]tetrahydrofuran-3,4-diyl diacetate (23): Starting from **10** (100 mg, 0.14 mmol) and **11** (41 mg, 0.14 mmol), the procedure described for **21** afforded **23** (53 mg, 56%) as an orange powder. M.p. 147 °C; $[\alpha]_D^{20} = +25.0$ ($c = 1.0$, THF); IR (KBr): $\tilde{\nu} = 3400, 2967, 2867, 1750, 1690, 1558, 1509, 1444, 1372, 1328, 1248, 1133, 1074, 844, 806, 702\text{ cm}^{-1}$; ^1H NMR (500 MHz, CD_3OD): $\delta = 8.75$ (d, $J = 0.7$ Hz, 1H), 8.50 (d, $J = 3.0$ Hz, 1H), 8.00–7.90 (m, 2H), 7.70–7.50 (m, 3H), 7.48 (d, $J = 3.0$ Hz, 1H), 7.29 (d, $J = 0.7$ Hz, 1H), 6.30 (d, $J = 5.1$ Hz, 1H), 5.76–5.70 (m, 1H), 5.68–5.62 (m, 1H), 4.48–4.42 (m, 1H), 4.05–3.80 (m, 6H), 2.10 (s, 3H), 2.06 (s, 3H); ^{13}C NMR (125 MHz, CD_3OD): $\delta = 171.47, 171.14, 170.14, 168.83, 164.47, 157.57, 150.26, 149.67, 149.62, 134.97, 133.65, 129.77, 128.90, 120.67, 116.09, 107.50, 98.42, 88.02, 83.85, 76.12, 72.52, 71.11, 70.64, 40.21, 20.52, 20.30$ (1 peak missing); HR-MS (FAB): calcd for $\text{C}_{29}\text{H}_{29}\text{N}_5\text{NaO}_{13}^+$ $[\text{M}+\text{Na}]^+$: 678.1659; found: 678.1646.

N-(2-[(2S,3R,4R,5R)-5-(6-Aminopurin-9-yl)-3,4-dihydroxytetrahydrofuran-2-yl]methoxy)ethyl]-2,3-dihydroxy-5-nitrobenzamide (1): A solution of **21** (48 mg, 0.07 mmol) in MeNH₂ (25% in EtOH, 5 mL) was stirred for 30 min at 20 °C. After evaporation in vacuo, the orange residue was dissolved in H₂O (10 mL) and extracted three times each with Et₂O (10 mL), toluene (10 mL), and CH₂Cl₂ (10 mL). After lyophilization from H₂O, **1** (29 mg, 82%) was obtained as a yellow powder and shown by analytical HPLC ($\text{H}_2\text{O}/\text{MeCN}/\text{CF}_3\text{COOH}$ 90:10:0.1 \rightarrow 40:60:0.1) to be pure. M.p. 141 °C; $[\alpha]_D^{20} = -16.0$ ($c = 1.0$, H₂O); IR (KBr): $\tilde{\nu} = 3422, 2944, 1639, 1556, 1500, 1472, 1422, 1333, 1261, 1122, 1072, 989, 828, 806, 700, 650, 556, 478, 406\text{ cm}^{-1}$; ^1H NMR (300 MHz, CD_3OD): $\delta = 8.48$ (d, $J = 3.3$ Hz, 1H), 8.45 (s, 1H), 8.18 (s, 1H), 7.50 (d, $J = 3.0$ Hz, 1H), 6.06 (d, $J = 5.0$ Hz, 1H), 4.69 (t, $J = 5.4$ Hz, 1H), 4.49 (t, $J = 5.4$ Hz, 1H), 4.22–4.20 (m, 1H), 3.84–3.65 (m, 6H); ^{13}C NMR (125 MHz, $\text{D}_2\text{O}+1$ drop CD_3OD): $\delta = 169.39, 156.83, 155.78, 153.12, 149.14, 148.47, 140.33, 133.03, 121.31, 119.21, 116.00, 108.74, 89.08, 84.70, 75.34, 71.37, 70.38, 70.18, 39.79$; HR-MS (FAB): calcd for $\text{C}_{19}\text{H}_{22}\text{N}_5\text{O}_9^+$ $[\text{MH}]^+$: 492.1479; found: 492.1460.

N-(2-[(2S,3R,4R,5R)-5-(4-Amino-2-oxo-1,2-dihydropyrimidin-1-yl)-3,4-dihydroxytetrahydrofuran-2-yl]methoxy)ethyl]-2,3-dihydroxy-5-nitrobenzamide (2): Starting from **22** (48 mg, 0.07 mmol), the procedure described for **1** gave **2** (28 mg, 82%) as an orange powder. M.p. 166 °C; $[\alpha]_D^{20} = +15.0$ ($c = 1.0$, CHCl_3); IR (KBr): $\tilde{\nu} = 3412, 3211, 2922, 2878, 1646, 1561, 1494, 1406, 1339, 1273, 1122, 1076, 989, 911, 789, 700, 600, 561\text{ cm}^{-1}$; ^1H NMR (500 MHz, D_2O): $\delta = 8.44$ (d, $J = 3.0$ Hz, 1H), 7.81 (d, $J = 7.6$ Hz, 1H), 7.66 (d, $J = 3.0$ Hz, 1H), 5.88 (d, $J = 4.0$ Hz, 1H), 5.68 (d, $J = 7.6$ Hz, 1H), 4.40–4.37 (m, 1H), 4.30–4.29 (m, 1H), 4.28–4.24 (m, 1H), 4.00 (d, $J = 9.5$ Hz, 1H), 3.90–3.60 (m, 5H); ^{13}C NMR (125 MHz, $\text{D}_2\text{O}+1$ drop of CD_3OD): $\delta = 169.83, 168.64, 166.67, 158.42, 149.10, 141.77, 132.77, 122.15, 116.60, 108.83, 96.62, 90.73, 83.91, 75.58, 70.52, 70.44, 70.03, 39.98$; HR-MS (FAB): calcd for $\text{C}_{18}\text{H}_{21}\text{N}_5\text{O}_{10}\text{Na}^+$ $[\text{M}+\text{Na}]^+$: 490.1186; found: 490.1176.

N-(2-[(2S,3R,4R,5R)-5-[4-(Benzoylamino)-6-oxo-1,6-dihydropyrimidin-1-yl]-3,4-dihydroxytetrahydrofuran-2-yl]methoxy)ethyl]-2,3-dihydroxy-5-nitrobenzamide (24): Starting from **23** (30 mg, 0.05 mmol), the procedure described for **1** provided **24** (21 mg, 80%) as an orange powder. M.p. 142 °C; $[\alpha]_D^{20} = +7.0$ ($c = 1.0$, CHCl_3); IR (KBr): $\tilde{\nu} = 3421, 2933, 2867, 1683, 1656, 1550, 1508, 1444, 1333, 1261, 1122, 989, 844, 806, 700, 556\text{ cm}^{-1}$;

¹H NMR (300 MHz, D₂O): δ = 8.56 (d, J = 0.7 Hz, 1H), 8.24 (d, J = 3.0 Hz, 1H), 7.80–7.70 (m, 2H), 7.63–7.50 (m, 3H), 7.28 (d, J = 3.0 Hz, 1H), 6.94 (d, J = 0.7 Hz, 1H), 5.91 (d, J = 2.1 Hz, 1H), 4.70–4.68 (m, 1H), 4.63–4.60 (m, 1H), 4.36–4.30 (m, 1H), 4.10–3.60 (m, 6H); ¹³C NMR (125 MHz, D₂O+1 drop of CD₃OD): δ = 169.89, 169.26, 168.82, 165.10, 156.64, 149.32, 148.84, 134.15, 133.27, 131.95, 129.79, 128.40, 122.13, 116.28, 107.74, 98.47, 91.86, 84.64, 76.35, 70.07, 69.95, 68.95, 40.46; HR-MS (FAB): calcd for C₂₅H₂₆N₅O₁₁⁺ [MH]⁺: 572.1629; found: 572.1645.

***N*-[2-[(2*S*,3*R*,4*R*,5*R*)-5-(4-Amino-6-oxo-1,6-dihydropyrimidin-1-yl)-3,4-dihydroxytetrahydrofuran-2-yl]methoxyethyl]-2,3-dihydroxy-5-nitrobenzamide (3)**: A solution of **24** (20 mg, 0.035 mmol) in NH₃ (25% in H₂O, 5 mL) and MeOH (5 mL) was stirred for 24 h at 55 °C and then evaporated in vacuo. The orange residue was dissolved in H₂O (10 mL) and extracted three times each with Et₂O (10 mL), toluene (10 mL) and CH₂Cl₂ (10 mL). After lyophilization from H₂O, **3** (29 mg, 82%) was obtained as an orange powder, which contained traces of benzamide. IR (KBr): $\tilde{\nu}$ = 3411, 3189, 2911, 2844, 2355, 1650, 1555, 1467, 1389, 1333, 1261, 1122, 1072, 977, 805, 716, 667 cm⁻¹; ¹H NMR (500 MHz, D₂O): δ = 8.40 (s, 1H), 7.90 (d, J = 2.7 Hz, 1H), 7.49 (d, J = 2.7 Hz, 1H), 5.90 (s, 1H); 5.45 (d, J = 4.9 Hz, 1H), 4.27 (d, J = 5.3 Hz, 1H), 4.22–4.18 (m, 1H), 4.15–4.05 (m, 1H), 3.98–3.50 (m, 6H); ¹³C NMR (125 MHz, [D₆]DMSO): δ = 169.03, 168.52, 167.32, 166.28, 166.23, 162.89, 160.54, 149.15, 120.80, 114.48, 104.01, 86.97, 82.57, 73.87, 70.07, 69.96, 69.58, 38.19; MS (ESI): m/z (%): 468 (10) [MH]⁺, 467 (39) [M]⁺, 466 (100) [M–H]⁺.

2,3-Dihydroxy-*N*-[2-[(3*aR*,4*R*,6*R*,6*aR*)-6-methoxy-2,2-dimethylperhydrofuro[3,4-*d*] [1,3]dioxol-4-yl]methoxyethyl]-5-nitrobenzamide (25): A mixture of **15** (0.10 g, 0.41 mmol), **11** (0.12 g, 0.41 mmol), and NEt₃ (0.18 mL, 1.20 mmol) in DMF (5 mL) was stirred under Ar for 4 h at 20 °C. Evaporation in vacuo and FC (SiO₂, CH₂Cl₂/acetone/HCOOH 79:20:1) provided **25** (0.13 g, 75%) as a yellow powder. M.p. 137 °C; $[\alpha]_D^{20}$ = –62.0 (c = 1.0, CHCl₃); IR (KBr): $\tilde{\nu}$ = 3400, 2989, 2944, 2856, 2344, 1650, 1561, 1511, 1472, 1350, 1322, 1278, 1161, 1100, 1039, 872, 816, 739, 656, 594 cm⁻¹; ¹H NMR (300 MHz, CDCl₃): δ = 8.24 (d, J = 2.7 Hz, 1H), 7.90 (d, J = 2.7 Hz, 1H), 7.62 (brs, 1H), 5.12 (s, 1H), 4.72 (d, J = 5.7 Hz, 1H), 4.64 (d, J = 5.7 Hz, 1H), 4.42 (t, J = 5.1 Hz, 1H), 3.71–3.50 (m, 6H), 3.38 (s, 3H), 1.48 (s, 3H), 1.31 (s, 3H); ¹³C NMR (50 MHz, CDCl₃): 226.30, 166.80, 152.87, 143.88, 137.22, 126.04, 111.19, 110.33, 107.89, 83.10, 82.84, 79.19, 69.93, 66.43, 52.63, 37.71, 24.00, 22.47; MS (FAB): m/z (%): 429 (74) [MH]⁺, 397 (100) [M–MeO]⁺; C₁₈H₂₄N₂O₁₀ (428.40): calcd: C 50.47, H 5.65, N 6.54; found: C 50.31, H 5.90, N 6.24.

2,3-Dihydroxy-5-nitro-*N*-[2-[(2*R*,3*R*,4*R*)-3,4,5-trihydroxytetrahydrofuran-2-yl]methoxyethyl]benzamide (4): A solution of **25** (0.10 g, 0.23 mmol) in H₂SO₄ (0.1N in H₂O, 1 mL) and H₂O (2 mL) was heated for 1 h at 100 °C. After cooling and neutralization with a saturated aqueous solution of BaCO₃ (pH control), the precipitated BaSO₄ was filtered off and the solvent was evaporated in vacuo. The solid residue was dissolved in H₂O (containing 1% of HCOOH, 10 mL) and extracted with EtOAc (3 × 20 mL). The combined organic layers were evaporated in vacuo to give **4** (mixture of anomers) (0.08 g, 91%) as a yellow solid. M.p. 87–90 °C; IR (KBr): $\tilde{\nu}$ = 3400, 2933, 1639, 1556, 1517, 1472, 1339, 1283, 1089, 894, 783, 744, 711, 656 cm⁻¹; ¹H NMR (300 MHz, CD₃OD, mixture of anomers): δ = 8.36 (d, J = 2.7 Hz, 1H), 7.74 (d, J = 2.7 Hz, 1H), 5.14 (d, J = 4.2 Hz, 1H), 4.14–4.09 (m, 1H), 4.02–3.95 (m, 2H), 3.86–3.84 (m, 1H), 3.74–3.59 (m, 5H); ¹³C NMR (125 MHz, CD₃OD, mixture of anomers): δ = 170.16, 156.70, 148.45, 141.09, 116.37, 116.08, 113.56, 103.57, 98.30, 83.37, 82.88, 77.24, 74.00, 72.77, 72.53, 72.48, 70.93, 70.86, 58.50, 40.90, 40.76; MS (FAB): m/z (%): 375 (100) [MH]⁺; HR-MS (FAB): calcd for C₁₄H₁₈N₂NaO₁₀⁺ [M+Na]⁺: 397.0859; found: 397.0824.

Molecular modeling: The design of the target molecules was carried out on Silicon Graphics Crimson and Indigo workstations. The starting geometries for the molecular mechanics studies were constructed with the program MOLOC^[25] from crystallographic data and standard molecular fragments. The proposed inhibitor was minimized separately and docked manually into its expected binding site. The coordinates of COMT and the Mg²⁺ ion were constrained. The inhibitors were minimized inside the enzyme. Energy minimizations were performed in vacuo by MOLOC with the MAB force field.^[25] The energy was minimized by conjugate gradients to a final value of the sum of the squares of the components of the gradient of less than the accuracy (0.1 or relative value of 1). The structures were visualized in Insight II^[26] as shown in the Figures 1a and 2a.

Enzymatic studies: **Materials**: Reagents were purchased from Fluka and Merck, Darmstadt. *S*-Adenosyl-L-[methyl-³H]methionine ([³H]SAM, specific activity: 15 Ci mmol⁻¹, The Radiochemical Centre, Amersham) was diluted with SAM (sulfate, *p*-toluenesulfonate, BioResearch, Liscate, Italy) to a specific activity 3.64 Ci mol⁻¹ and to a concentration 5.5 mmol L⁻¹. Dithiothreitol (DTT) was obtained from Calbiochem-Behring Corp., Luzern, and 2-(4-*tert*-butylphenyl)-5-(4'-biphenyl)-1,3,4-oxadiazole (butyl-PBD) from Novartis, Basel.

Wistar rats were killed by decapitation and the liver removed. The tissue was homogenized in ice-cold water (1:10 *w/v*) containing 0.2% Triton X-100 and 0.002% dithiothreitol (triton/DTT) and then centrifuged at 12000 g for 20 min at 4 °C. Supernatants were further diluted (1:10) with Triton/DTT solution.

Kinetic measurements: IC₅₀ values were determined as follows: The inhibitors were dissolved in Me₂SO as 1.2 mM stock solution and further diluted with 0.001N HCl. The reactions were performed in standard polyethylene scintillation vials. 25 μ L of the inhibitor in varying concentrations from 10⁻⁴ to 10⁻⁶ mol L⁻¹ were mixed with 250 μ L freshly prepared buffer–substrate mixture consisting of 200 μ L potassium phosphate buffer (0.1 mol L⁻¹, pH 7.6), 10 μ L MgCl₂ (0.1 mol L⁻¹), 15 μ L substrate (benzene-1,2-diol, 0.05 mol L⁻¹), 10 μ L dithiothreitol (0.065 mol L⁻¹), 5 μ L deionized H₂O, and 10 μ L [³H]SAM (5.5 mmol L⁻¹, specific activity: 3.64 Ci mol⁻¹). Then 25 μ L of tissue extract were added. The reaction was started by incubating the vials in a water-bath at 37 °C for 15 min. The incubation was stopped by adding 250 μ L HOAc (5.7%) containing guaiacol (0.1 g L⁻¹) and 3 mL of scintillation fluid (5 g butyl-PBD, dissolved in 200 mL toluene, made up to 1 L with *n*-hexane) was added. The vials were capped and more than 98% [³H]guaiacol formed was extracted into the organic phase by vigorous shaking for 1 min. The samples were counted in a Beckmann LS 6000 TA scintillation counter. IC₅₀ values were determined with and without preincubation in the presence of inhibitor. Enzyme preparations were preincubated for 15 min at 37 °C at varying inhibitor concentrations from 10⁻⁴ to 10⁻⁶ mol L⁻¹ in the presence of buffer mixture without the substrate benzene-1,2-diol in the case of the inhibitor **5**. In the case of the potential bisubstrate inhibitors, preincubation without the substrates benzene-1,2-diol and SAM was performed.

For the determination of K_M and K_I values, either the concentration of the substrate benzene-1,2-diol was varied between 28 μ M and 500 μ M at saturating SAM concentration (183 μ M) or the concentration of SAM was varied between 10 μ M and 183 μ M at saturating benzene-1,2-diol concentration (2.5 mM). The volumes of all reagents were doubled and the incubation time varied between 1 min and 15 min at 37 °C with and without preincubation in the presence of inhibitor. 10 mL of scintillation fluid was added, the samples were shaken for 5 min and centrifuged. The aqueous phase was frozen by placing the samples in dry ice/acetone, and the organic phase was poured into a scintillation vial and counted.

A dialysis experiment was performed as follows: The inhibitors were incubated with the enzyme preparation at 37 °C for 15 min in the presence of SAM and MgCl₂. Dialysis of the incubation mixture against 0.01 M KH₂PO₄/K₂HPO₄ buffer, pH 7.6, which contained 0.003 M MgCl₂ and 100 mg DTT in 10 L buffer was performed, and the relative inhibition was determined after 0, 2, 4, 6, 8, and 24 h. The loss of activity owing to degradation of the enzyme was measured in the same experiment.

Acknowledgment

This work was supported by F. Hoffmann-La Roche, Basel, and a doctoral fellowship from the “Studienstiftung des Deutschen Volkes” to B.M. We thank Dr. C. Thilgen (ETH Zürich) for assistance with the nomenclature.

- [1] P. T. Mannistö, I. Ulmanen, K. Lundström, J. Taskinen, J. Tenhunen, C. Tilgmann, S. Kaakkola, *Prog. Drug Res.* **1992**, *39*, 291–350.
- [2] D. R. Jeffery, J. A. Roth, *Biochemistry* **1987**, *26*, 2955–2958.
- [3] Y.-J. Zheng, T. C. Bruice, *J. Am. Chem. Soc.* **1997**, *119*, 8137–8145.
- [4] J. Borgulya, H. Bruderer, K. Bernauer, G. Zürcher, M. Da Prada, *Helv. Chim. Acta* **1989**, *72*, 952–968.

- [5] R. Bäckström, E. Honkanen, A. Pippuri, P. Kairisalo, J. Pystynen, K. Heinola, E. Nissinen, I.-B. Lindén, P. T. Mannistö, S. Kaakola, P. Pohto, *J. Med. Chem.* **1989**, *32*, 841–846.
- [6] J. Borgulya, M. Da Prada, R. Dingemanse, B. Scherschlicht, B. Schläppi, G. Zürcher, *Drugs of the Future* **1991**, *16*, 719–721.
- [7] R. A. Perez, E. Fernandez-Alvarez, O. Nieto, F. J. Piedrafita, *J. Med. Chem.* **1992**, *35*, 4584–4588.
- [8] E. Nissinen, I.-B. Lindén, E. Schultz, P. Pohto, *Arch. Pharmacol.* **1992**, *346*, 262–266.
- [9] R. T. Borchardt, *J. Med. Chem.* **1980**, *23*, 347–357.
- [10] R. T. Borchardt, J. A. Huber, Y. S. Wu, *J. Med. Chem.* **1976**, *9*, 1094–1099.
- [11] J. K. Coward, D. J. Bussolotti, C.-D. Chang, *J. Med. Chem.* **1974**, *17*, 1286–1289.
- [12] R. Borchardt, Y. S. Wu, *J. Med. Chem.* **1976**, *19*, 1099–1103.
- [13] O. W. Lever, Jr., C. Hyman, H. L. White, *J. Pharm. Sci.* **1984**, *73*, 1241–1244.
- [14] E. K. Yau, J. K. Coward, *J. Org. Chem.* **1990**, *55*, 3147–3158.
- [15] G. L. Anderson, D. L. Bussolotti, J. K. Coward, *J. Med. Chem.* **1981**, *24*, 1271–1277.
- [16] a) P. M. Woster, A. Y. Black, K. J. Duff, J. K. Coward, A. E. Pegg, *J. Med. Chem.* **1989**, *32*, 1300–1307; b) M. R. Burns, J. K. Coward, *Bioorg. Med. Chem.* **1996**, *4*, 1455–1470.
- [17] K. Hinterding, P. Hagenbuch, J. Rétey, H. Waldmann, *Chem. Eur. J.* **1999**, *5*, 227–236.
- [18] E. Benghiat, P. A. Crooks, R. Goodwin, F. Rottman, *J. Pharm. Sci.* **1986**, *75*, 142–145.
- [19] E. Benghiat, P. A. Crooks, *J. Med. Chem.* **1983**, *26*, 1470–1477.
- [20] F. K. Winkler, F. Hoffmann-La Roche, Basel, unpublished results, **1994**.
- [21] J. Vidgren, L. A. Svensson, A. Liljas, *Nature* **1994**, *368*, 354–358.
- [22] P. Y. S. Lam, P. K. Jadhav, C. J. Eyermann, C. N. Hodge, Y. Ru, L. T. Bacheler, J. L. Meek, M. J. Otto, M. M. Rayner, Y. N. Wong, C.-H. Chang, P. C. Weber, D. A. Jackson, T. R. Sharpe, S. Erickson-Viitanen, *Science* **1994**, *263*, 380–384.
- [23] a) U. Obst, V. Gramlich, F. Diederich, L. Weber, D. W. Banner, *Angew. Chem.* **1995**, *107*, 1874–1877; *Angew. Chem. Int. Ed. Engl.* **1995**, *34*, 1739–1742; b) U. Obst, D. W. Banner, L. Weber, F. Diederich, *Chem. Biol.* **1997**, *4*, 287–295.
- [24] a) S. H. Reich, S. E. Webber, *Perspect. Drug Discovery Des.* **1993**, *1*, 371–390; b) H. J. Böhm, G. Klebe, H. Kubinyi, *Wirkstoffdesign, Spektrum, Heidelberg*, **1996**; c) H. Kubinyi, *J. Recept. Signal. Trans. Res.* **1999**, *19*, 15–39.
- [25] P. R. Gerber, K. Müller, *J. Comput. Aided Mol. Design* **1995**, *9*, 251–268.
- [26] Insight II User Guide, October 1997, San Diego, Molecular Simulations Inc., **1997**.
- [27] W. C. Still, MacroModel V. 6.0, Columbia University, New York, **1998**.
- [28] H. Vorbrüggen, K. Krolikiewicz, B. Bennua, *Chem. Ber.* **1981**, *114*, 1234–1255.
- [29] H. Vorbrüggen, B. Bennua, *Chem. Ber.* **1981**, *114*, 1279–1286.
- [30] H. Vorbrüggen, G. Höfle, *Chem. Ber.* **1981**, *114*, 1256–1268.
- [31] H. Vorbrüggen, K. Krolikiewicz, *Angew. Chem.* **1975**, *87*, 417; *Angew. Chem. Int. Ed. Engl.* **1975**, *14*, 421–422.
- [32] S. Pitsch, *Helv. Chim. Acta* **1997**, *80*, 2286–2314.
- [33] A. Bolliger, F. Reuter, *J. Proc. R. Soc. NSW* **1938**, *72*, 329–334.
- [34] T. W. Greene, P. G. M. Wuts, *Protective Groups in Organic Synthesis*, Wiley, New York, **1991**.
- [35] G. M. Visser, J. van Westrenen, C. A. A. van Boeckel, J. H. van Boom, *Recl. Trav. Chim. Pays-Bas* **1986**, *105*, 528–537.
- [36] W. Traube, *Ann. Chem. Pharm.* **1904**, *331*, 64–88.
- [37] D. J. Brown, *J. Soc. Chem. Ind. London* **1950**, *69*, 353–356.
- [38] G. Zürcher, M. Da Prada, *J. Neurochem.* **1982**, *38*, 191–195.
- [39] E. Schultz, E. Nissinen, *Biochem. Pharmacol.* **1989**, *38*, 3953–3956.
- [40] J. F. Morrison, *Trends Biochem. Sci.* **1982**, 102–105.
- [41] W. C. Bowmann, M. J. Rand, *Textbook of Pharmacology*, Blackwell Scientific, London, **1980**.
- [42] T. Lotta, J. Vidgren, C. Tilgmann, I. Ulmanen, K. Melén, I. Julkunen, J. Taskinen, *Biochemistry* **1995**, *34*, 4202–4210.
- [43] I. A. Pearl, D. L. Beyer, *J. Am. Chem. Soc.* **1955**, *77*, 3660–3662.

Received: August 10, 1999 [F1968]